Geomechanics and Engineering, *Vol. 8, No. 3 (2015) 323-359*
DOI: http://dx.doi.org/10.12989/gae.2015.8.3.323

The ground response curve of underwater tunnels, excavated in a strain-softening rock mass

Ahmad Fahimifar [1a], Hamed Ghadami [*2] and Masoud Ahmadvand [3b]

[1] *Department of Civil and Environmental Engineering, Amirkabir University of Technology, 424 Hafez Ave, Tehran, Iran*
[2] *Department of Civil Engineering, Science and Research Branch, Islamic Azad University, Tehran, Iran*
[3] *Department of Civil Engineering, Tafresh University, First of Tehran road, Tafresh, Iran*

(*Received December 28, 2013, Revised November 25, 2014, Accepted December 02, 2014*)

Abstract. This paper presents an elasto-plastic model for determination of the ground response curve of a circular underwater tunnel excavated in elastic-strain softening rock mass compatible with a nonlinear Hoek–Brown yield criterion. The finite difference method (FDM) was used to propose a new solution to calculate pore water pressure, stress, and strain distributions on periphery of circular tunnels in axisymmetric and plain strain conditions. In the proposed solution, a modified non-radial flow pattern, for the hydraulic analysis, is utilized. To evaluate the effect of gravitational loads and variations of pore water pressure, the equations concerning different directions around the tunnel (crown, wall, and floor) are derived. Regarding the strain-softening behavior of the rock mass, the stepwise method is executed for the plastic zone in which parameters of strength, dilatancy, stresses, strains, and deformation are different from their elasto-plastic boundary values as compared to the tunnel boundary values. Besides, the analytical equations are developed for the elastic zone. The accuracy and application of the proposed method is demonstrated by a number of examples. The results present the effects of seepage body forces, gravitational loads and dilatancy angle on ground response curve appropriately.

Keywords: ground response curve; gravitational loads; seepage; strain-softening behavior; underwater tunnel

1. Introduction

Convergence-confinement method is the most commonly frequently applied approach for tunnel design and analysis. Using this approach, the ground response curve (the relationship between the decreasing internal pressure and increasing radial displacement) is determined based on ground convergence to the internal pressure of the tunnel and ground behavior is demonstrated based on this curve during the tunnel excavation. The solutions presented for ground response analysis are categorized in two groups: closed-form analytical solutions and unclosed numerical-analytical solutions. Because of the occasional application of a large number of

*Corresponding author, Ph.D. Candidate, E-mail: hamed.ghadami@yahoo.com
[a] Professor, E-mail: fahim@aut.ac.ir
[b] MS.c., E-mail: m.ahmadvand@taha-ce.com

Copyright © 2015 Techno-Press, Ltd.
http://www.techno-press.org/?journal=gae&subpage=7 ISSN: 2005-307X (Print), 2092-6219 (Online)

simplifying assumptions, the closed-form solutions are considered as approximate, while unclosed analytical-numerical approaches yield more accurate solutions since they evaluate rock mass behavior using a more sophisticated approach.

When tunnel excavation is performed below the water table, tunnel behavior can be affected by the seepage. When tunnel excavation is performed below the water table, tunnel behavior can be affected by the seepage. Tunnels below groundwater table can be either sealed or drained. Sealed tunnel does not influence the groundwater condition and in situ water pressure is completely absorbed by the lining. Thus, a heavier support is required; otherwise, the lining element may fail causing failure of the rock mass surrounding the tunnel. In fact, based on the convergence-confinement method, it is important to note that most of the loading should be carried by the rock and not by the lining. On the other hand, in a drained tunnel, a seepage flow will be developed. The seepage flow and the pore water pressure, developed around the tunnel, affect the responses of the lining and of the rock mass significantly. In a tunnel with permeable lining below groundwater table, the effective stress law must be applied in the analysis. In this condition, the applied inward seepage body forces are generated by the hydarulic gradients (Fahimifar *et al*. 2015).

As compared to a tunnel in a dry condition, the induced inward seepage loads in a tunnel below groundwater table (underwater tunnel) increase the tunnel convergence significantly. Therefore, to design underwater tunnels, it is required to perform a powerful analysis taking into account the hydro-mechanical aspects of tunnelling.

Once the plastic zone is developed around the tunnel periphery, the gravitational forces induced by the weight of plastic zone affect the response curve significantly. In fact, gravitational loading differs for various directions around the tunnel periphery, and, for the same internal pressure, convergence of the crown is expected to be larger than that of the walls and floor, because of the weight of the failed material on the top of the tunnel.

To derive ground response curve of circular tunnels, a number of analytical solutions have been proposed based on the brittle-plastic and perfectly plastic behavior models and considering linear Mohr-Coulomb failure criterion and nonlinear Hoek-Brown failure criterion (Brown *et al*. 1983, Detournay and Fairhurst 1987, Wang 1996, Carranza-Torres and Fairhurst 1999, Sharan 2003, 2005, Carranza-Torres 2004, Park and Kim 2006).

Brown *et al*. (1983), Alonso *et al*. (2003), Park *et al*. (2008), and Lee and Pietruszczak (2008) proposed analytical-numerical elastoplastic methods considering the strain-softening behavior for determination of the ground response curve; however, the effect of gravitational and seepage loads have not been taken into account in these approaches.

Brown and Bray (1982), Lee *et al*. (2006), Shin *et al*. (2007) and Fahimifar *et al*. (2014) considered the effects of seepage and pore water pressure in their solutions; nevertheless, study of the analytical approaches reveal that the effective stress has not been received adequate attention, since the analyses are performed based on the total stress. It must be noted that rock mass strength, stress fields, and deformation are, indeed, controlled by effective stress and seepage body forces. Fernandez (1994), Fahimifar and Zareifard (2009), Shin *et al*. (2010, 2011) presented their analytical models considering effective stress (rather than total stress) and seepage body forces. Through the Fernandez (1994) method, an elastic analysis was proposed by considering the seepage body forces. In addition, Fahimifar and Zareifard (2009) proposed a novel elastoplastic solution for analysis of the underwater tunnels taking into account the rock mass strain-softening behavior. In this model, seepage was modeled using a combination of Kolymbas accurate seepage model (Kolymbas and Wagner 2007) (for elastic zone) and radial seepage model, taking into account the hydromechanical coupling for the rock mass (in the plastic zone).

Shin *et al*. (2010, 2011) proposed a new elastoplastic model on the basis of Mohr-Coulomb failure criterion regarding the brittle-plastic behavior; however, despite their complexity, these methods do not provide a solution for computing the pore water pressure distribution. One of the few proposed solutions for tunnel analysis in which the gravitational loadings are taken into account is the one presented by Zareifard and Fahimifar (2012).

In the present research, an elastoplastic model is proposed for determination of ground response curve by considering the seepage body forces and gravitational loads. In this regard stress, strain, and pore water pressure are determined at different directions at the tunnel periphery. Considering the axisymmetric condition, for calculating stress, strain, and deformation at different directions of tunnel periphery, the body forces induced by gravitational loads and the pore water pressure in a given direction are generalized to all directions around the tunnel and then boundary conditions are applied. Therefore, simultaneous study of the effect of these two factors (pore water pressure and gravitational loads) leads to more accurate results as compared to those of other methods.

2. Model assumption and governing equations

Fig. 1 illustrates an underwater tunnel with radius of r_0 under internal pressure of P_i in a rock mass with initial uniform effective stress of σ'_θ and uniform hydrostatic pressure of P_{wo}. As shown in Fig. 1, two different zones may be formed around the tunnel: the external elastic zone, and the internal plastic zone, which may be divided into the softening zone and the residual zone.

As tunnel excavation initiates, a non-uniform pore water pressure is developed from the tunnel boundary to the radius of R_w, named as seepage radius. As the radial distance increases from R_w, water pressure indicates no change.

Fig. 1 shows the seepage forces and stress components on each abcd rock mass element around the tunnel. Considering the equilibrium relationship in radial direction for element abcd, Eq. (1) is obtained as follows

$$\begin{aligned}&\left(\sigma'_r+\frac{\partial\sigma'_r}{\partial r}\partial r\right)(r+\partial r)\partial\theta-\sigma'_r r\partial\theta-\left(\sigma'_\theta+\frac{\partial\sigma'_\theta}{\partial\theta}\partial\theta\right)\partial r\sin\frac{\partial\theta}{2}-\sigma'_\theta\partial r\sin\frac{\partial\theta}{2}\\&+\left(\sigma'_{r\theta}+\frac{\partial\sigma'_{r\theta}}{\partial\theta}\partial\theta\right)\partial r\cos\frac{\partial\theta}{2}-\sigma'_{r\theta}\partial r\cos\frac{\partial\theta}{2}+(Fs_r+Fg_r)r\partial r\partial\theta=0\end{aligned}\tag{1}$$

Where, σ'_r: effective radial stress; σ'_θ: effective circumferential stress; Fs_r: seepage body force in radial direction; and Fg_r is body force induced by gravitational loads in radial direction.

A similar equation is also obtained for circumferential direction. Assuming $\partial\theta$ as an infinitesimal value and simplifying Eq. (1), the equilibrium equations in radial and circumferential directions are obtained as Eqs. (2)-(3)

$$\frac{\partial\sigma'_r}{\partial r}+\frac{1}{r}\frac{\partial\sigma'_{r\theta}}{\partial\theta}-\frac{(\sigma'_\theta-\sigma'_r)}{r}+Fg_r+Fs_r=0\tag{2}$$

$$\frac{1}{r}\frac{\partial\sigma'_\theta}{\partial r}+\frac{\partial\sigma'_{r\theta}}{\partial\theta}+\frac{2\sigma'_{r\theta}}{r}+Fg_\theta+Fs_\theta=0\tag{3}$$

In Eqs. (2)-(3), Fs_r and Fs_θ, are the seepage body forces in radial and circumferential directions,

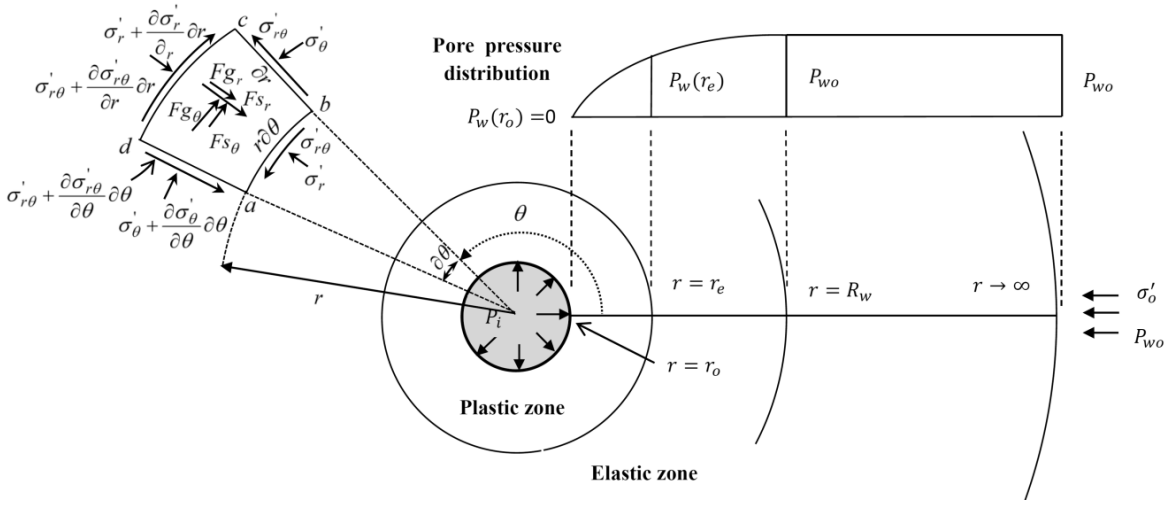

Fig. 1 Geometry of the problem

respectively and are expressed as Eqs. (4)-(5)

$$Fs_r = i_r \gamma_w \tag{4}$$

$$Fs_\theta = i_\theta \gamma_w \tag{5}$$

Where, i_r and i_θ are hydraulic gradients in r and θ directions, respectively, and γ_w is specific weight of the water.

Also, in Eqs. (2)-(3), Fg_r and $Fg_{\theta,}$ are the body forces induced by gravitational loads in the plastic zones, and are expressed as

$$Fg_r = \gamma \sin\theta \tag{6}$$

$$Fg_\theta = \gamma \cos\theta \tag{7}$$

Where, γ is the saturated specific weight of the rock mass.

As Fg_r and Fg_θ are gravitational body forces induced by the weight of fractured rock mass in the plastic zone, the seepage body forces (Eqs. (4)-(5)) are only considered in the analysis of the elastic zone.

Obtaining an exact elasto-plastic analytical solution for Eqs. (2)-(3) is extremely complicated and even impossible in more cases, because the principal effective stresses may rotate in each direction. For simplifying the problem, a number of assumptions are made:

Through the axisymmetric condition all quantities such as geometry, initial field stresses and pore water pressure are assumed as independent of θ. Thus, u_θ, $\sigma'_{r\theta}$, γ_{rz}, and $\gamma_{\theta z}$ will be zero. To evaluate the effect of gravitational loads and variations of pore water pressure, the equations were derived for various directions around the tunnel (crown, wall, and floor). For each direction, boundary conditions and the applied loads were generalized to all directions because of the axisymmetric conditions. Terzaghi's effective stress equation ($\sigma' = \sigma - Pw$) is applied for the rock mass (Terzaghi 1923), which is true in practical applications, as confirmed by the experimental

studies (Skempton 1961). Assuming plane strain condition, $\varepsilon_z = \gamma_{rz} = 0$. Considering these simplifications, the equilibrium relationship through radial direction is simplified as Eq. (8)

$$\frac{\partial \sigma'_r}{\partial r} - \frac{(\sigma'_\theta - \sigma'_r)}{r} + Fg_r + Fs_r = 0 \tag{8}$$

Under axisymmetric condition, deformation-strain relationships are expressed by Eqs. (9)-(11): (Timoshenko and Goodier 1982)

$$\varepsilon_r = -\frac{du}{dr} \tag{9}$$

$$\varepsilon_\theta = -\frac{u}{r} \tag{10}$$

$$\frac{d\varepsilon_\theta}{dr} = \frac{\varepsilon_r - \varepsilon_\theta}{r} \tag{11}$$

Where, u indicates radial deformation and, ε_r and ε_θ denote radial and circumferential strains, respectively.

3. Hydraulic analysis

In this research, the seepage model proposed by Ming *et al*. (2010) is used. Ming *et al*. (2010) presented a seepage model for underwater tunnels using conformal mapping. This model is highly efficient in analysis of shallow to deep tunnels under different conditions, since it produces separate equations in two cases of constant hydraulic head and constant pore water pressure at the tunnel surface; besides it considers exact boundary conditions. The proposed model is based on the following assumptions:

- The circular tunnel is in a saturated, homogeneous and isotropic aquifer.
- The flow is in steady state.
- Water pressure is considered as constant at the tunnel surface.
- No change is induced in the groundwater table because of seepage flow

Fig. 2 shows the geometry of Ming's model. In the case that pore water pressure is constant at the tunnel surface, pore water pressure distribution in Ming's model can be expressed in all directions around the tunnel in terms of (r, θ) coordinates as Eq. (12) (Fahimifar *et al*. 2014)

$$\begin{aligned} P_w(r,\theta) &= (h - r\sin\theta)\gamma_w \\ &+ \frac{P_w(r_o,\theta) + \gamma_w r_o \sin\theta - \gamma_w h}{2\ln\left(\frac{h}{r_o} - \sqrt{\left(\frac{h}{r_o}\right)^2 - 1}\right)} \left(\ln \frac{(r\cos\theta)^2 + \left(r\sin\theta - h + \sqrt{h^2 - {r_o}^2}\right)^2}{(r\cos\theta)^2 + \left(r\sin\theta - h - \sqrt{h^2 - {r_o}^2}\right)^2} \right) \end{aligned} \tag{12}$$

Also, hydraulic head distribution is obtained from the Bernoulli's equation

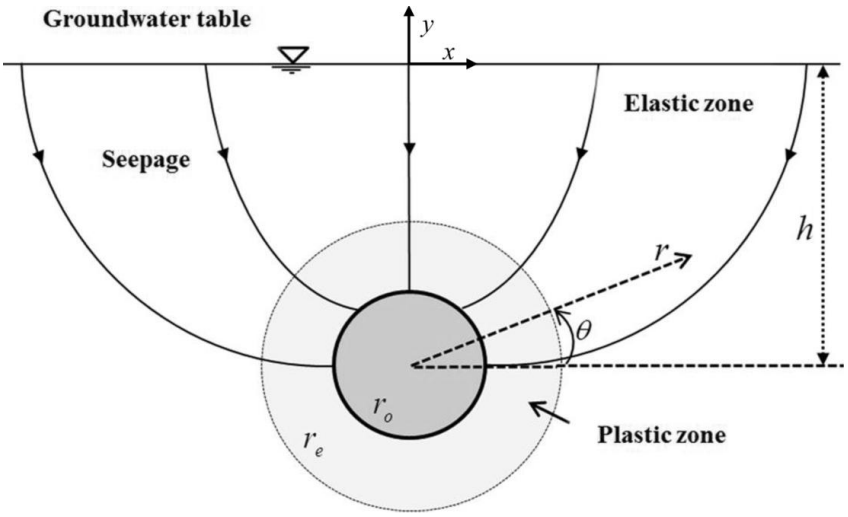

Fig. 2 Geometry of the seepage model

$\left(H_w = y + \frac{P_w}{\gamma_w} = r\sin\theta - h + \frac{P_w}{\gamma_w} \right)$ as

$$H_w(r,\theta) = \frac{P_w(r_o,\theta)/\gamma_w + r_o\sin\theta - h}{2\ln\left(\frac{h}{r_o} - \sqrt{\left(\frac{h}{r_o}\right)^2 - 1}\right)} \left(\ln \frac{(r\cos\theta)^2 + \left(r\sin\theta - h + \sqrt{h^2 - r_o^2}\right)^2}{(r\cos\theta)^2 + \left(r\sin\theta - h - \sqrt{h^2 - r_o^2}\right)^2} \right) \tag{13}$$

4. Behavior model

The rock mass is assumed to exhibit strain-softening behavior, which can be reduced to the perfect elasto-plastic or elasto-brittle-plastic cases. In the strain-softening behavior model, the rock mass will behave as elastic until the failure criterion is satisfied. Then, the rock mass strength gradually decreases and reaches its residual strength. Such behavior is generally characterized by a failure criterion and a plastic potential function (Fig. 3).

The gradual transition from an initial failure criterion to a residual failure criterion is controlled by a softening parameter. In the present study, the deviatoric plastic strain $\eta = \varepsilon_\theta^p - \varepsilon_r^p$ is employed as the softening parameter. Although there is no universal approach for defining the strain-softening parameter, the above mentioned softening parameter (Alonso et al. 2003) is the most widely accepted one.

Here, the Mohr-Coulomb criterion is used as plastic potential function for a non-associated flow rule. For the Mohr-Coulomb type of plastic potential function, the relation between the plastic parts of the radial and circumferential strain increments is obtained as follows (Alonso *et al*. 2003): (Fig. 3)

$$\Delta\varepsilon_r^p = -K\Delta\varepsilon_\theta^p \tag{14}$$

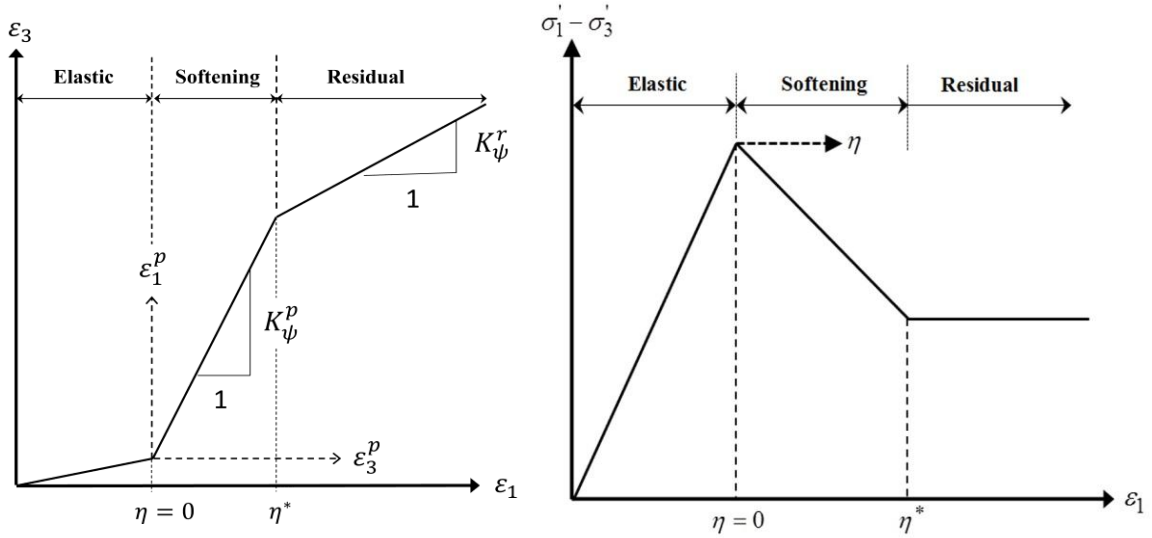

(a) (b)

Fig. 3 Strain-softening behavior model (Alonso *et al*. 2003)

Where, $K\psi$ is the dilation factor, and is given as (Alonso *et al*. 2003)

$$K = \frac{1+\sin\psi}{1-\sin\psi} \tag{15}$$

In Eq. (15), ψ is the dilation angle and varies as a function of the softening parameter η.

The rock mass is assumed to obey the Hoek-Brown failure criterion, given by: (Hoek and Brown 1980)

$$\sigma_\theta' - \sigma_r' = \left\{ m\sigma_r'\sigma_c + s\sigma_c^2 \right\}^a \tag{16}$$

In which, $\sigma_1' = \sigma_\theta'$ and $\sigma_3' = \sigma_r'$ are the major and minor principal stresses at the failure, respectively; σ_c is the uniaxial compression strength of the intact rock; m and s are strength parameters of the rock mass; and a is exponential coefficient related to the Hoek-Brown failure criterion. In this research, a is considered as 0.5.

In contrast to the solution presented by Brown *et al*. (1983), the solution proposed in this work considers the elastic strains induced in the plastic zone. Therefore, total strain is divided into two parts, elastic and plastic strains

$$\begin{Bmatrix} \varepsilon_r \\ \varepsilon_\theta \end{Bmatrix} = \begin{Bmatrix} \varepsilon_r^e \\ \varepsilon_\theta^e \end{Bmatrix} + \begin{Bmatrix} \varepsilon_r^p \\ \varepsilon_\theta^p \end{Bmatrix} \tag{17}$$

It should be noted that in the plastic zone, the failure and dilation parameters (m, s and ψ), appearing in Eqs. (15)-(16), can be described by a bilinear function based on the deviatoric plastic strain η (Alonso *et al*. 2003)

$$w=\begin{cases} w_p-(w_p-w_r)\dfrac{\eta(i)}{\eta^*} & 0<\eta<\eta^* \\ w_r & \eta>\eta^* \end{cases} \tag{18}$$

Where w represents one of the parameters m, s and ψ, and η^* is the critical deviatoric plastic strain from which the residual behavior starts, and should be identified by experiments. The subscripts 'p' and 'r' denote the peak and residual values, respectively.

A comparison between the equations produced by two strain-softening models (i.e., Alonso *et al*. 2003, Brown *et al*. 1983) revealed that the parameter η^* can be estimated as Eq. (19): (Park *et al*. 2008)

$$\eta^*=(\alpha-1)\varepsilon_\theta(r_e) \tag{19}$$

Where, α is a parameter indicating the length of strain-softening zone in the method of Brown *et al*. (1983).

5. Analysis of the plastic zone

By substituting the seepage body forces and gravitational loads in Eq. (8), Eq. (20) is derived as follows

$$\frac{d\sigma'_r}{dr}+\gamma_w\frac{dH_w}{dr}-\gamma\sin\theta=\frac{\sigma'_\theta-\sigma'_r}{r} \tag{20}$$

By substituting the Hoek-Brown failure criterion in right hand of Eq. (20), one can derive the equilibrium equation in the plastic zone as Eq. (21)

$$\frac{d\sigma'_r}{dr}+\gamma_w\frac{dH_w}{dr}-\gamma\sin\theta=\frac{\{m\sigma'_r\sigma_c+s{\sigma_c}^2\}^{\frac{1}{2}}}{r} \tag{21}$$

Since functions $-\gamma\sin\theta$ and $\gamma_w\dfrac{dH_w}{dr}$ depend on the direction angle, different equilibrium equations are derived for different directions at tunnel periphery.

As mentioned, unlike Brown *et al*. (1983) model, which considers unchanged elastic strain throughout the plastic zone, the model proposed in this work considers the increment of elastic strain separately. The relationships between the elastic strain increments and the effective stress increments σ'_r and σ'_θ are given by Hook's law (Timoshenko and Goodier 1982)

$$\begin{Bmatrix}\Delta\varepsilon_r^e(i)\\ \Delta\varepsilon_\theta^e(i)\end{Bmatrix}=\frac{1}{2G}\begin{bmatrix}1-\nu & -\nu\\ -\nu & 1-\nu\end{bmatrix}\begin{Bmatrix}\Delta\sigma'_r(i)\\ \Delta\sigma'_\theta(i)\end{Bmatrix} \tag{22}$$

Since a multi-linear behavior model and the incremental theory of plasticity have been used, the governing equations on the stresses and strains in the plastic zone have no analytical solutions, and must be solved numerically, as presented in Appendix A.

6. Analysis of the elastic zone

To estimate the effective stress in the elastic zone, the superposition principle is used, through which the total effective stress in the elastic zone is composed of the sum of initial ground stress $(\sigma'_r, \sigma'_\theta)$, the extra stress induced by the tunnel excavation $(\sigma'_{r(e)}, \sigma'_{\theta(e)})$ and the extra stress induced by seepage body forces $(\sigma'_{r(s)}, \sigma'_{\theta(s)})$

$$\sigma'_r = \sigma'_{r(in)} + \sigma'_{r(e)} + \sigma'_{r(s)} \tag{23}$$

$$\sigma'_\theta = \sigma'_{\theta(in)} + \sigma'_{\theta(e)} + \sigma'_{\theta(s)} \tag{24}$$

In addition, ground deformation, due to excavation and seepage through the radial direction is obtained from the sum of radial deformations induced by both excavation and the seepage

$$u_r = u_{r(e)} + u_{r(s)} \tag{25}$$

Before excavating the tunnel, the rock mass is in uniform equilibrium state. To simulate this situation, the elastic deformation and strains of rock mass induced by initial hydrostatic field stress σ'_o under axisymmetric and plane strain conditions are calculated using Eqs. (26)-(27)

$$u_{r(in)} = -\frac{1+\upsilon}{E}\sigma'_o(1-2\upsilon)r \tag{26}$$

$$\varepsilon_{r(in)} = -\varepsilon_{\theta(in)} = -\frac{1+\upsilon}{E}\sigma'_o(1-2\upsilon) \tag{27}$$

In this regard, the initial ground stresses are determined using Eq. (28)

$$\sigma'_{r(in)} = \sigma'_{\theta(in)} = \sigma'_o \tag{28}$$

It must be noted that, initial deformation and strains, derived from Eqs. (26)-(27), are not incorporated in the calculation of total deformation and strains induced by the excavation and seepage (Fahimifar *et al*. 2015).

6.1 Stresses and strains induced by the seepage in the elastic zone

Governing equilibrium equation derived on the basis of induced stresses by the seepage is expressed as Eq. (29)

$$\frac{\partial\sigma'_{r(s)}}{\partial r} - \frac{(\sigma'_{\theta(s)} - \sigma'_{r(s)})}{r} + Fs_r = 0 \tag{29}$$

Where, Fs_r is the seepage body force in radial direction and is expressed as Eq. (4) ($Fs_r = i_r\gamma_w$). Substituting $i_r = \frac{dH_w}{dr}$ in Eq. (29), Eq. (30) is obtained

$$\frac{\partial' \sigma'_{r(s)}}{\partial r} - \frac{(\sigma'_{\theta(s)} - \sigma'_{r(s)})}{r} + \gamma_w \frac{dH_w}{dr} = 0 \tag{30}$$

The plain strain condition between the stresses and strains induced by the seepage is controlled by Hook's law for the elastic zone (Timoshenko and Goodier 1982)

$$\sigma'_{r(s)} = \frac{E_r}{(1+\nu_r)(1-2\nu_r)}\left[(1-\nu_r)\varepsilon_{r(s)} + \nu_r \varepsilon_{\theta(s)}\right] \tag{31}$$

$$\sigma'_{\theta(s)} = \frac{E_r}{(1+\nu_r)(1-2\nu_r)}\left[(1-\nu_r)\varepsilon_{\theta(s)} + \nu_r \varepsilon_{r(s)}\right] \tag{32}$$

Where, E and υ are elasticity modulus and Poisson's ratio of elastic rock mass, respectively.

Substituting Eqs. (31)-(32) into Eq. (30), Eq. (33) is derived for calculating the deformation induced by seepage in the elastic zone

$$\frac{d^2 u_{r(s)}}{dr^2} + \frac{1}{r}\frac{du_{r(s)}}{dr} - \frac{u_{r(s)}}{r^2} = B\gamma_w \frac{dH_w}{dr} \tag{33}$$

where

$$B = \frac{(1+\upsilon)(1-2\upsilon)}{E(1-\upsilon)} \tag{34}$$

Taking into account appropriate boundary conditions in a given direction, stresses, strains and deformations induced by the seepage body forces are derived by solving the differential Eq. (33) (see details in Appendix B).

6.2 Stresses and strains induced by the tunnel excavation in the elastic zone

During the tunnel excavation, excess stresses are induced due to the excavation of the surrounding rock mass. The governing equilibrium relationship for this induced stresses (ignoring the seepage body forces) is obtained as Eq. (35)

$$\frac{\partial \sigma'_{r(e)}}{\partial r} - \frac{(\sigma'_{\theta(e)} - \sigma'_{r(e)})}{r} = 0 \tag{35}$$

In the elastic zone, Hook's law is valid for the plain strain condition between the stresses and strains induced by the excavation (Timoshenko and Goodier 1982).

$$\sigma'_{r(e)} = \frac{E_r}{(1+\nu_r)(1-2\nu_r)}\left[(1-\nu_r)\varepsilon_{r(e)} + \nu_r \varepsilon_{\theta(e)}\right] \tag{36}$$

$$\sigma'_{\theta(e)} = \frac{E_r}{(1+\nu_r)(1-2\nu_r)}\left[(1-\nu_r)\varepsilon_{\theta(e)} + \nu_r \varepsilon_{r(e)}\right] \tag{37}$$

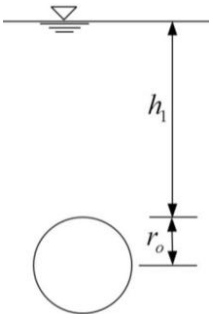

Fig. 4 Groundwater height

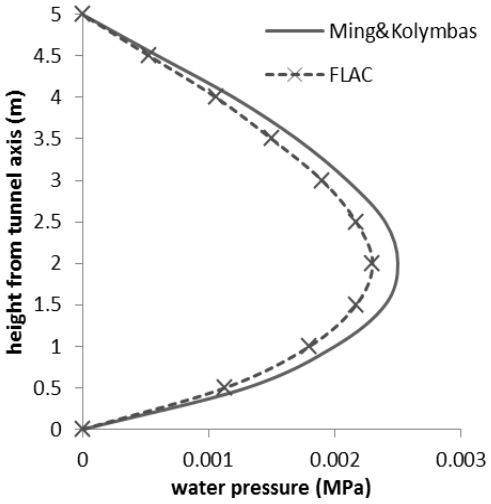

(a) Shallow tunnel ($h_1 / r_0 = 1$)

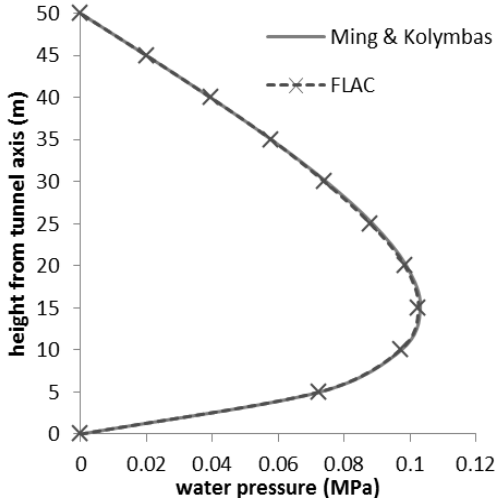

(b) Semi-shallow tunnel ($h_1 / r_0 = 10$)

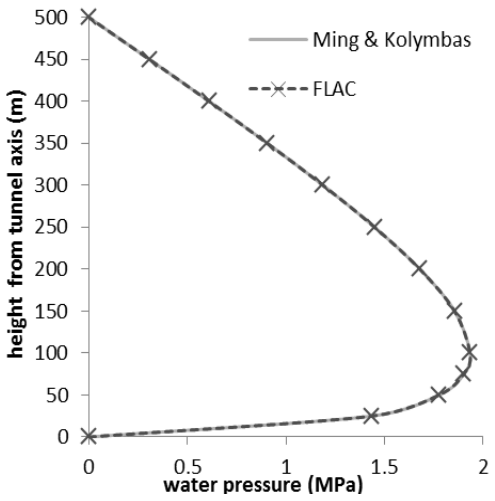

(c) Deep tunnel ($h_1 / r_0 = 100$)

Fig. 5 Pore water distribution through the vertical direction above the tunnel

Substituting Eqs. (36)-(37) into Eq. (35), Eq. (38) is derived for calculating deformation induced by excavation

$$\frac{d^2u_{r(e)}}{dr^2}+\frac{1}{r}\frac{du_{r(e)}}{dr}-\frac{u_{r(e)}}{r^2}=0 \tag{38}$$

Taking into account the appropriate boundary conditions through the considering direction, stresses, strains and deformations induced by the tunnel excavation are derived by solving the differential Eq. (38). (see details in Appendix C).

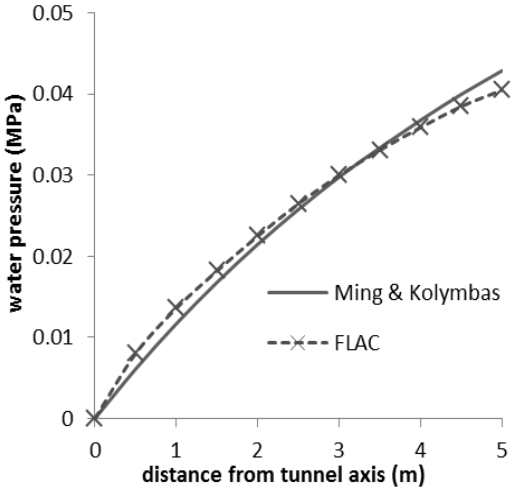

(a) Shallow tunnel ($h_1 / r_0 = 1$)

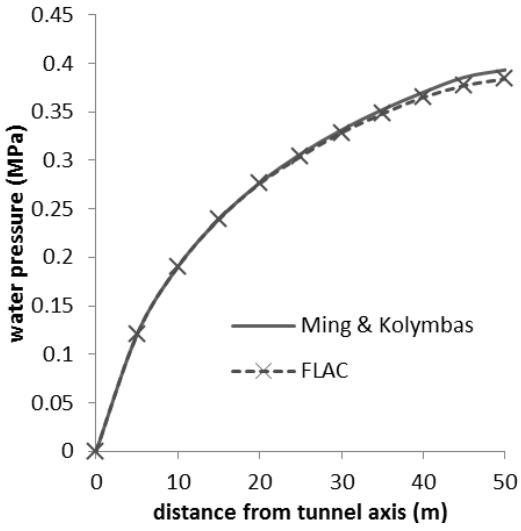

(b) Semi-shallow tunnel ($h_1 / r_0 = 10$)

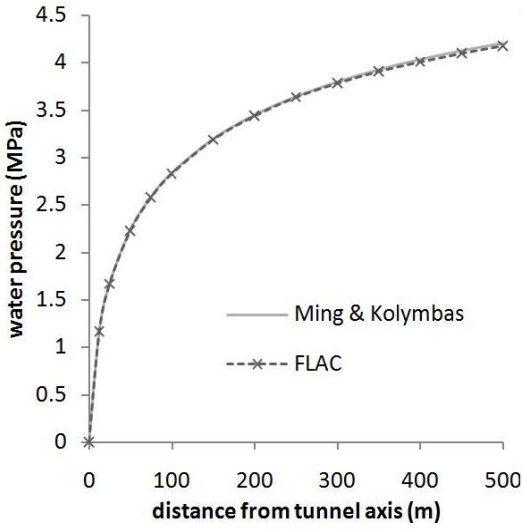

(c) Deep tunnel ($h_1 / r_0 = 100$)

Fig. 6 pore water distribution through horizontal direction for shallow tunnel

7. Validation of the proposed model

The solution presented in this paper has been programmed using MATLAB code. The proposed solution and the computer code are used to analyze several typical tunnels, and the results obtained are compared with those obtained from other models. Also, the effect of various parameters on ground response curve is examined using the model proposed.

7.1 Example 1

An underwater tunnel with radius of 5 m is excavated. Using the analytical Ming and Kolymbas (Kolymbas and Wagner 2007) seepage models as well as numerical FLAC program, pore water pressure around the tunnel periphery is analyzed under various groundwater conditions: shallow ($h_1 / r_0 = 1$), semi-shallow ($h_1 / r_0 = 10$), and deep ($h_1 / r_0 = 100$). Where, h_1 is the groundwater height from the tunnel crown (Fig. 4). Pore water pressure at the tunnel surface is considered as zero.

Here, it must be noted that despite the different procedure and formulation of the methods proposed by Ming *et al*. (2010) and Kolymbas and Wagner (2007), the results obtained by these two methods are in complete agreement in all direction at tunnel periphery for shallow to deep tunnels.

Fig. 5 shows water pressure distribution along the vertical axis at tunnel crown for shallow to deep tunnels for Ming and Kolymbas models and the FLAC program. For shallow tunnels, Ming and Kolymbas models give overestimate values in comparison to those of FLAC; as the results of these two models are 8% greater than those of FLAC.

Fig. 6 presents pore water distributions through horizontal direction for shallow to deep tunnels for Ming and Kolymbas models and FLAC program which are almost the same for Ming *et al*. (2010) and Kolymbas and Wagner (2007) and FLAC program.

Fig. 7 illustrates pore water distribution through vertical directions at floor of the tunnel for shallow to deep tunnels is shown for Ming and Kolymbas models and FLAC program. As shown in the figure, the obtained results are almost the same for Ming and Kolymbas model and FLAC program.

Considering the results obtained through Figs. 5-7, Ming *et al*. (2010) and Kolymbas and Wagner (2007) models are of acceptable accuracy for computation of pore water pressure distribution around underwater tunnels in various directions for various depths.

7.2 Example 2

In this example, the proposed method is compared with Park *et al*. (2008) model and Brown *et al*. (1983) model in dry conditions (tunnel above the groundwater level). The data set used in Park's model is shown in Table 1.

Figs. 8-10 exhibit ground response curve, radial and circumferential stresses using the proposed method, Park *et al*. (2008) and Brown *et al*. (1983) models. As the number of loops are selected large enough ($n > 5{,}000$), the results obtained by the proposed method are consistent with those of Park's model. To evaluate the effect of elastic strain increment in the plastic zone, a comparison was made between the results obtained from the proposed method and Park's model compared to those of Brown's model.

Brown *et al*. (1983) neglected the elastic strain distribution in the plastic zone, while the

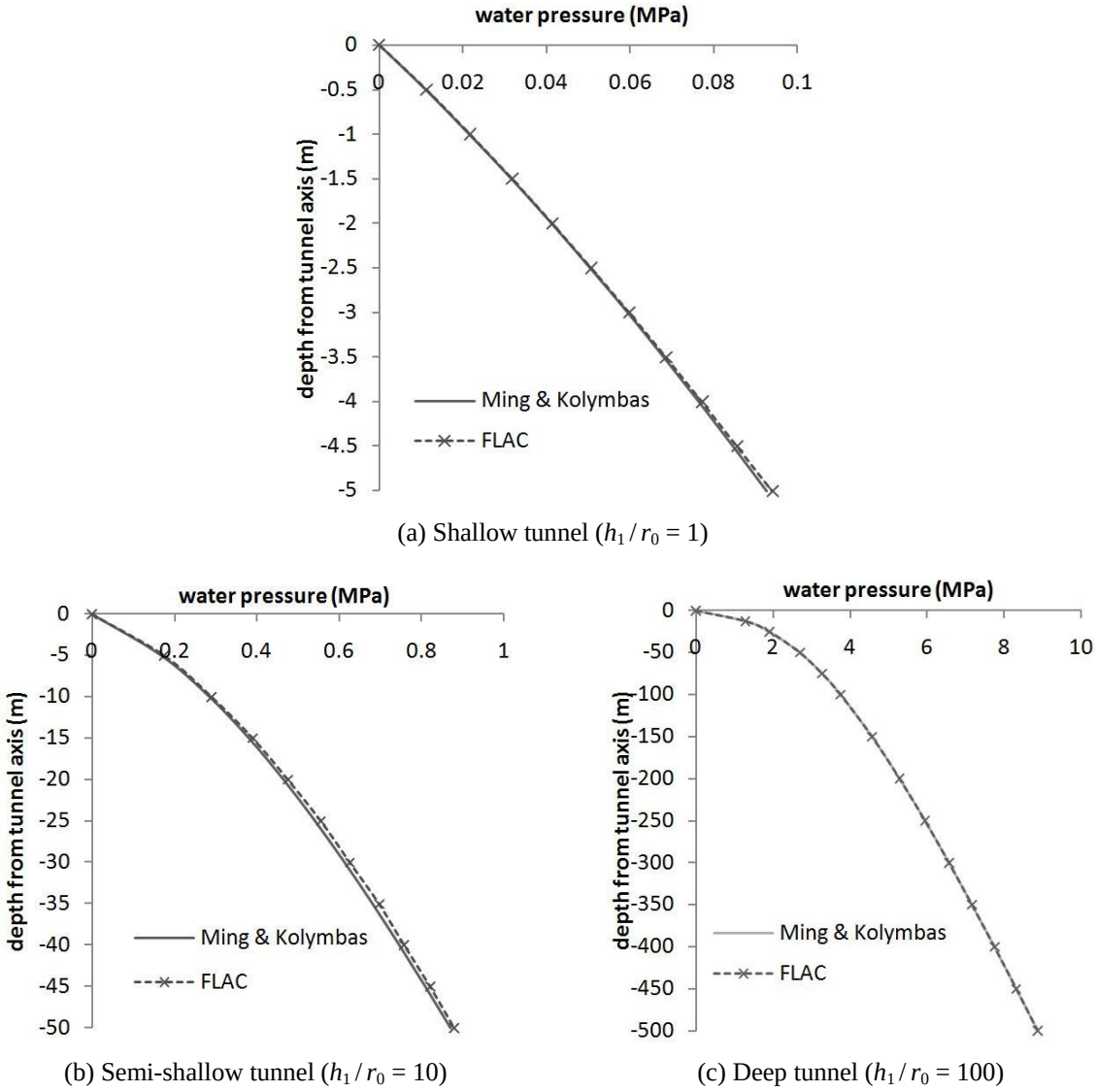

(a) Shallow tunnel ($h_1 / r_0 = 1$)

(b) Semi-shallow tunnel ($h_1 / r_0 = 10$)

(c) Deep tunnel ($h_1 / r_0 = 100$)

Fig. 7 pore water distribution through vertical direction at tunnel floor

Table 1 Data set of Park's model (Park *et al*. 2008)

Parameter	Value	Parameter	Value	Parameter	Value
E	1380	m_p	0.5	σ_o	3.31 MPa
Y	0.25	s_p	0.001	P_i	0
σ_c	27.6 MPa	m_r	0.1	a	0.5
ϕ_p	30	s_r	0	η^*	0.004742
r_o	5.35 m	ψ_p	19.47	ψ_r	5.22

proposed method and Park's model (Park *et al*. 2008) consider the effects of elastic strain increment and dilatancy angle in the plastic zone. As shown in Figs. 8-10, using the proposed method and Park's model, compared to Brown's model, greater values for elasto-plastic radius and ground convergence are obtained. In this regard, the elasto-plastic radius and convergence of the tunnel increase from 12.41 and 0.89 m for Brown's model to 19.58 and 0.276 m in the proposed model (for ψ_p = 19.47 and ψ_r = 5.22), respectively. Considering the increasing peak and residual dilatancy angles from 0 to 19.47° and 0 to 5.22°, respectively, the elasto-plastic radius rises from 18.62 to 19.58 m while the tunnel convergence enhances from 0.176 to 0.2765 m, respectively. Based on these findings, Brown *et al*. (1983) model gives underestimate values for the ground convergence and the elasto-plastic radius.

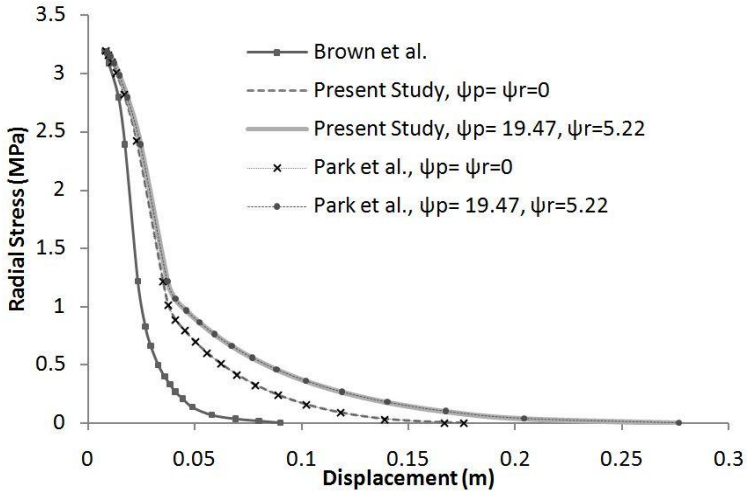

Fig. 8 Comparison of the ground response curves of tunnel wall (θ = 0) using the proposed method, Park's model, and Brown's model (example 2)

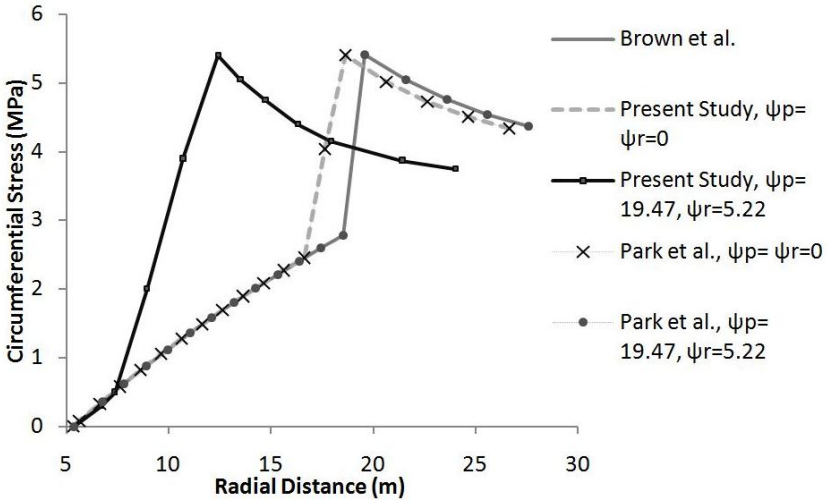

Fig. 9 Comparison of the circumferential stress using the proposed method (θ = 0), Park's model, and Brown's model (example 2)

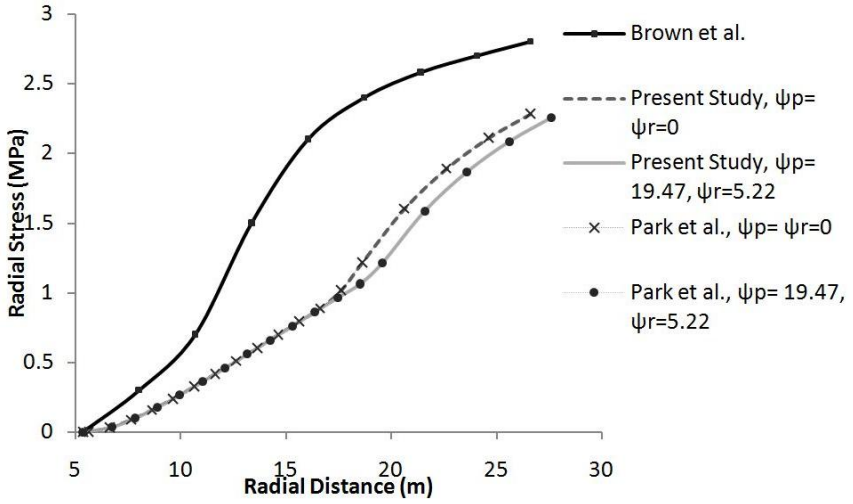

Fig. 10 Comparison of radial stress using the proposed method $\theta = 0$, Park's model, and Brown's model (example 2)

Table 2 Data set of Zareifard's model (Zareifard and Fahimifar 2012)

Parameter	Value	Parameter	Value	Parameter	Value
E	4000	m_p	0.3	σ_o	10 MPa
υ	0.25	s_p	0.0001	P_i	0.5
σ_c	30 MPa	m_r	0.1	A	0.5
γ	28 KN/m^3	s_r	0	η^*	0.004
r_o	3 m	ψ_p	0	ψ_r	0

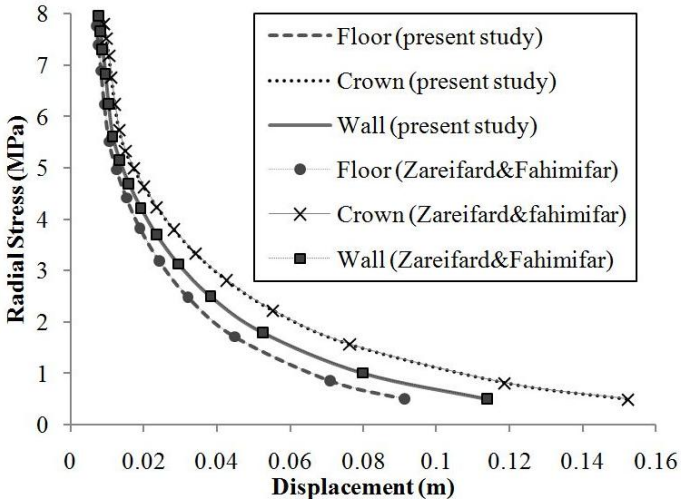

Fig. 11 Comparison of the ground response curves using the proposed method and Zareifard's model (example 3)

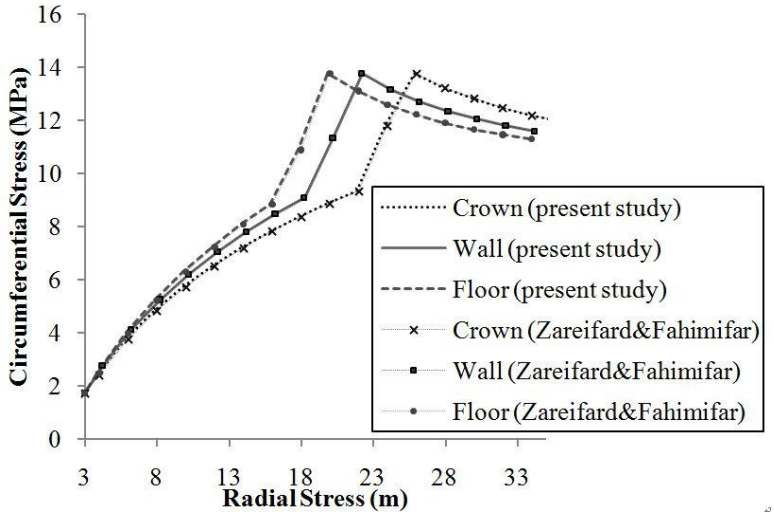

Fig. 12 Comparison of the circumferential stresses using the proposed method and Zareifard's model (example 3)

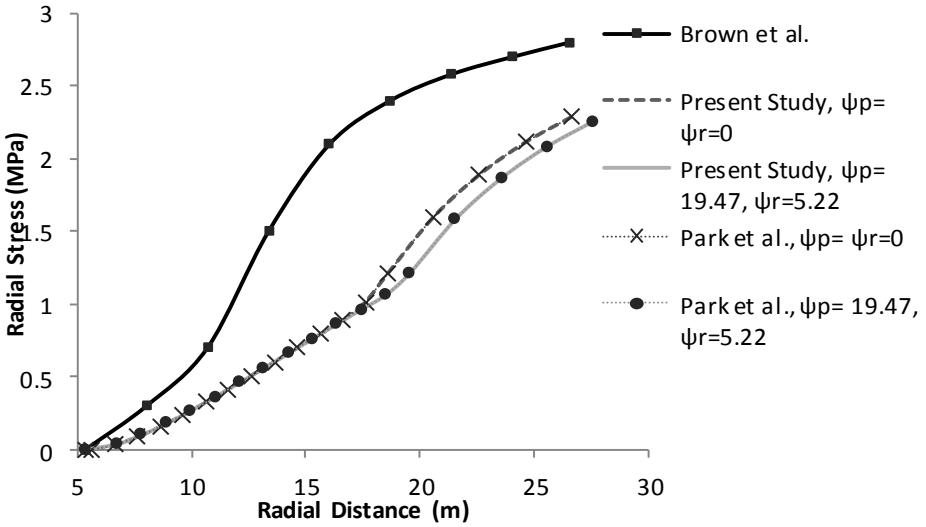

Fig. 13 Comparison of the radial stresses using the proposed method and Zareifard's model (example 3)

7.3 Example 3

In this example, the effect of gravitational loads in the plastic zone is examined. The model proposed in this work was compared to the one presented by Zareifard and Fahimifar (2012) by taking into account the effect of gravitational loads induced by fractured zone weight in dry condition (ignoring the seepage effects). In this regard, a tunnel with the following characteristics is considered.

Ground response curve, radial and circumferential stresses are evaluated using two model. The

results obtained from these two models are fitted with high accuracy. Taking into account the effect of gravitational loads, tunnel convergence and elastoplastic radius increase from floor to the crown of the tunnel. Therefore, the gravitational loads act as an instability factor in the crown and as a stability factor in the floor, respectively. However, these loads have no effect on tunnel's walls.

7.4 Example 4

As shown in Table 3, a tunnel is considered in a rock mass consisting of mudstone and siltstone at a depth of 300 m from the groundwater table. Based on these characteristics, Brown and Bray (1982) analyzed the given tunnel and reported the results.

Stress and strain in the Brown and Bray's model (Brown and Bray 1982) are analyzed using total stress in the equilibrium equations, ignoring the separate analysis of the body forces. Besides, the effects of dilatancy angle and elastic strain increment are ignored in the plastic zone, while the radial seepage forces are applied.

On the other hand, in the model proposed by Fahimifar and Zareifard (2009), despite taking into account the seepage body forces and more accurate analysis in the elastic zone by using the

Table 3 Data set of Brown and Bray method (Brown and Bray 1982)

Parameter	Value	Parameter	Value	Parameter	Value
E	20000 MPa	m_p	0.65	σ_o	27 MPa
υ	02	s_p	0.2	P_i	1.98 MPa
σ_c	40 MPa	m_r	0.2	r_o	3.0 m
ϕ_c	30	s_r	0.0001	h	300 m
a	0.5	P_{wo}	2.3 MPa		

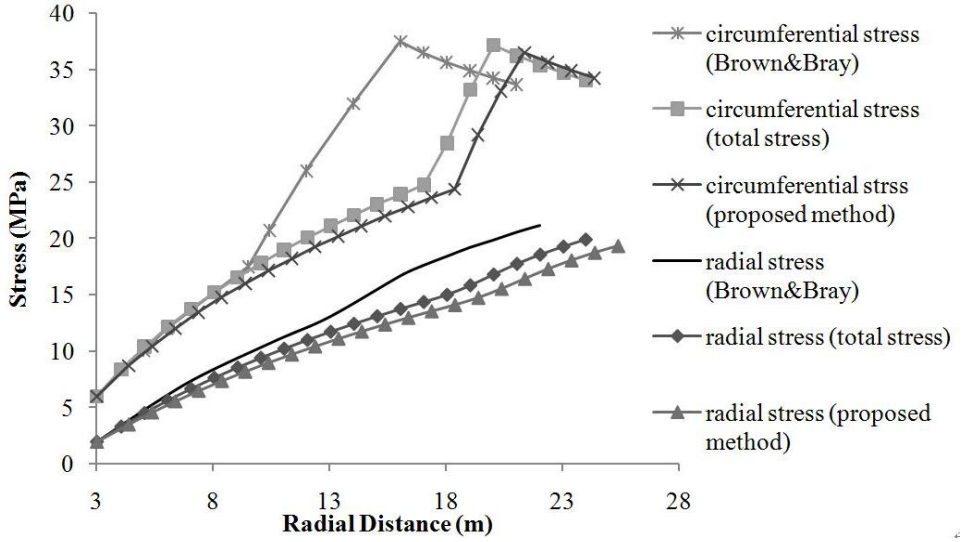

Fig. 14 Comparison of radial and circumferential stresses using the proposed method (θ = 0), total stress method, and Brown& Bray method (example 4)

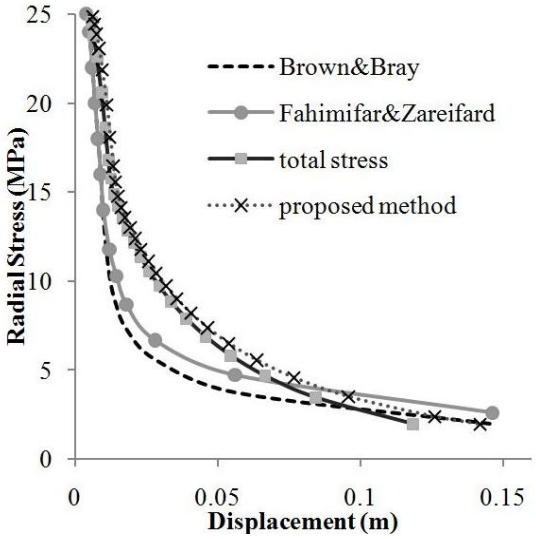

Fig. 15 Comparison of the ground response curves of tunnel wall ($\theta = 0$) using proposed method, total stress method, and Brown & Bray method (example 4)

non-radial seepage model of Kolymbas and Wagner (2007), the effects of dilatancy angle and elastic strain increment were not considered in the plastic zone. However in the proposed method, not only the seepage body forces are considered using the accurate seepage model of Ming et al. (2010), but the elastic strain increment is also calculated in the plastic zone with respect to the dilatancy angle, and the effects of these angle variations on the tunnel performance in the plastic zone are also taken into account.

Fig. 14 illustrates variations of σ_θ and σ_r versus radial distance based on Brown & Bray method, total stress method, and the proposed method. In addition, the ground response curves obtained on basis of Brown and Bray (1982), Fahimifar and Zareifard (2009), total stress methods, and the method proposed in this work are shown in Fig. 15. As the elastic strain increment in the plastic zone is applied in the proposed method and in the total stress method, greater values are obtained for the elasto-plastic radius as compared to Brown and Bray method. Since, the seepage body forces and the effective stresses are considered separately in the proposed method (unlike the total stress method), greater ground convergence and elasto-plastic radius are obtained. In this respect, for a constant dilatancy angle ($\psi = 0$) the ground convergence and the elasto-plastic radius are

Table 4 Characteristics of the studied tunnel

Parameter	Value	Parameter	Value	Parameter	Value
E	4000	m_p	0.3	σ_o	10 MPa
υ	0.25	s_p	0.0001	P_i	0.5
σ_c	30 MPa	m_r	0.1	a	0.5
γ	28 KN/m^3	s_r	0	η^*	0.004
r_o	3 m				

0.1185 m and 20.0439 m, respectively for total stress method and 0.142 m and 21.3649 m, respectively for the proposed method.

The range of seepage radius (R^2) (external radius of the rock zone affected by the seepage) in the Brown and Bray (1982) method was 150 m while it was considered as infinite in the Fahimifar and Zareifard (2009) method. In this example, this range was considered as equal to the groundwater level (300 m) using the proposed method. However, the variation of R_w affects the elasto-plastic radius and convergence of the tunnel; as in the proposed method, the change in R_w from 150 m to infinite, leads to an increase at the elasto-plastic radius and convergence of the tunnel from 21.096 m and 0.138 m to 22.00 m and 0.1524 m, respectively.

8. Effective parameters on ground response curve

In this part, effects of the variation of different parameters on the ground response curve are examined. Table 4 presents characteristics of the studied tunnel.

Fig. 16 indicates effect of dilatancy angle on ground response curve by keeping other parameters unchanged. An increase in dilatancy angle from 0 to 15° results in an increase in the ground convergence from 0.1116 to 0.454 m. In addition, by considering varying peak and residual dilatancy angles equal to 15 and 0°, respectively, the tunnel tends to show a behavior similar to that of 15° dilatancy angle in the vicinity of elastoplastic boundary (strain softening zone) and a behavior similar to that of 0° dilatancy angle in the zone at the vicinity of tunnel boundary (residual zone) and would have convergence of 0.1645 m.

Fig. 17 indicates ground response curve of the crown, wall, and floor of the underwater tunnel. As shown in the figure, considering the effect of gravitational loads, ground convergence varies from 0.0894 m at the tunnel wall to 0.1055 and 0.0778 m at its crown and floor, respectively. Thus, the gravitational loads lead to an 18% increase in the crown convergence and a 14% decrease in the floor convergence as compared to the wall convergence.

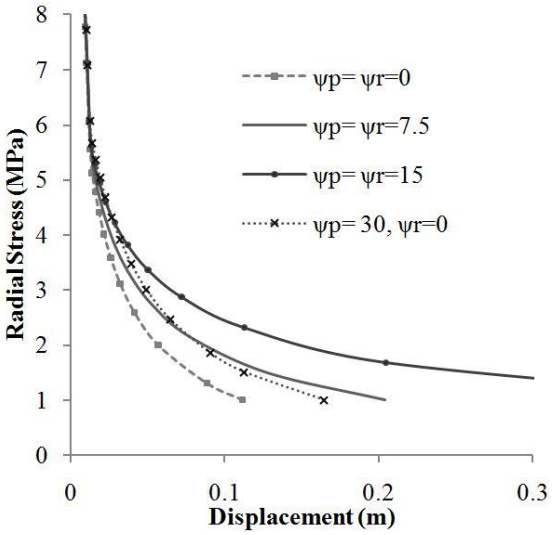

Fig. 16 The effect of dilatancy angle on GRC of tunnel wall (h = 300 m, $R_w = \infty$)

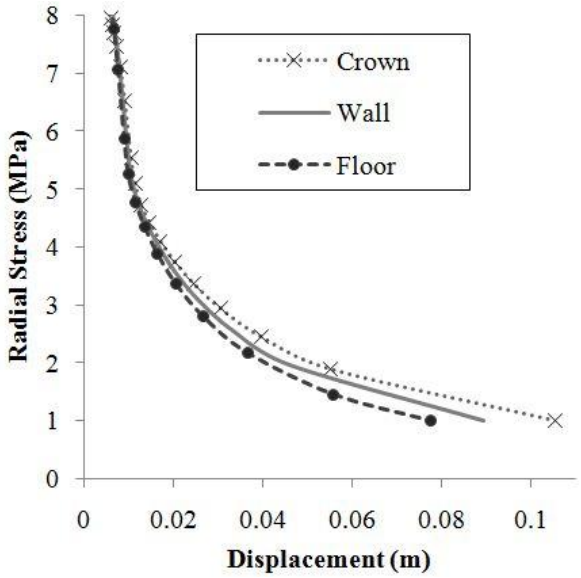

Fig. 17 GRC of crown, wall and floor (The effect of gravitational loads) (h = 300 m, R_w = 300 m, $\psi_p = \psi_r = 7.5°$)

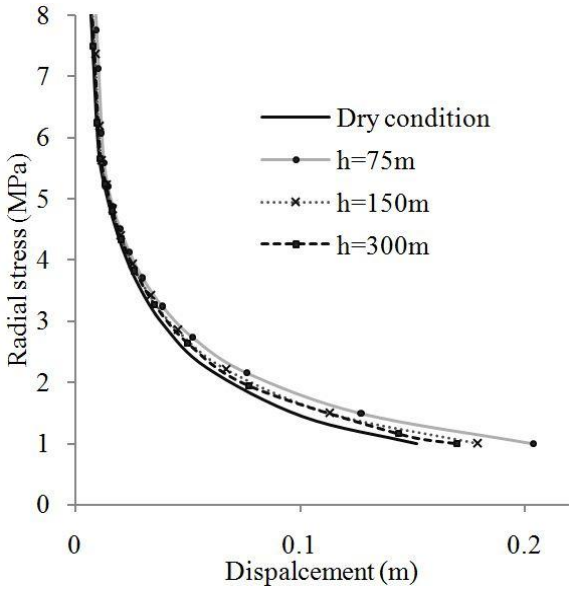

Fig. 18 The effect of groundwater height on GRC of tunnel wall ($R_w = \infty$, $\psi_p = \psi_r = 7.5°$)

Fig. 18 shows the effect of groundwater height on the ground response curve. As shown in the figure, an increase in water height from dry condition to 300 m results in an increase in the tunnel convergence from 0.1697 m to 0.2037 m.

Fig. 19 shows the effect of variations in seepage radius (the external boundary subject to the seepage) on the ground response curve. In the case, in which a zone is considered under effect of

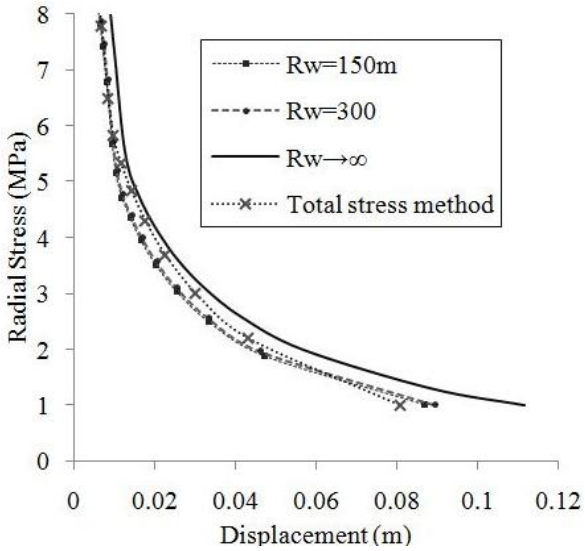

Fig. 19 The effect of seepage radius on GRC of tunnel wall (h = 300 m, $\psi_p = \psi_r$ = 7.5°)

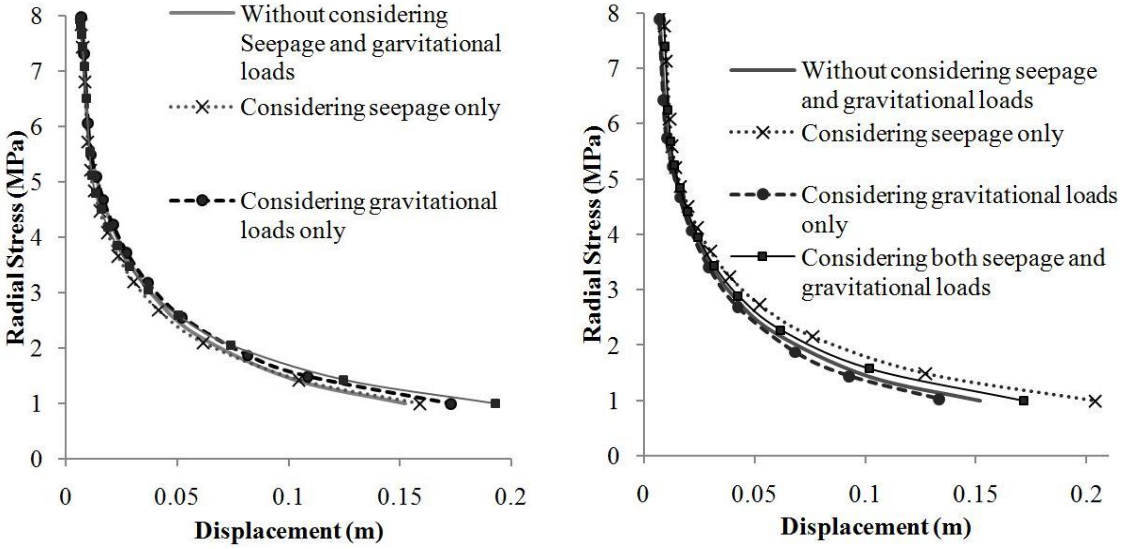

(a) Crown (b) Floor

Fig. 20 The effect of seepage and gravitational loads on GRC of tunnel ($\psi_p = \psi_r$ = 7.5°)

infinite seepage, clearly, greater values are obtained for tunnel convergence and the elastoplastic radius, as compared to a finite seepage radius and the total stress method (Fahimifar *et al*. 2014).

Fig. 20 illustrates ground response curve for the tunnel crown and floor, considering different conditions. As the figure shows, both seepage and gravitational loads lead to increase the convergence and thus the instability of the tunnel crown. Since, the maximum seepage radius for the vertical direction above the tunnel is considered as the groundwater height ($R_w = h$), the

seepage is of less significance on the ground response curve in comparison to the gravitational loads. Simultaneous effect of two seepage and gravitational loads leads to an increase in tunnel convergence from 0.1578 m to 0.1928 m. At tunnel floor, seepage and gravitational loads result in an increase and a decrease in tunnel convergence, respectively. However, in the case in which seepage radius in vertical direction at the tunnel floor is assumed as infinite, seepage effect outweighs the gravitational loads and the convergence increases from 0.1578 to 0.1726 m by simultaneous consideration of both factors. On the other hand, if seepage radius is assumed as finite, effect of gravitational loads outweighs the seepage, and the tunnel convergence reduces from 0.1578 to 0.135 m by simultaneous consideration of both parameters as compared to the initial conditions (ignoring the effects of seepage and gravitational loads).

9. Conclusions

In this paper, an analytical-numerical solution for determination of ground response curve of a circular underwater tunnel excavated in a Hoek-Brown strain-softening rock mass was presented, considering the seepage body forces and gravitational loads. The problem is considered in axial-symmetry condition and thus, the initial stress state was assumed to be hydrostatic. Through the developed previous seepage models, a more accurate model was proposed for calculation of pore water pressure and hydraulic head distribution in all directions around underwater tunnels. The proposed model compared and validated with several analytical elastoplastic models of tunnel under dry and saturated conditions. The concluding remarks are summarized as follows:

- The results clearly revealed that more accurate investigation of ground response curve of a circular underwater tunnel is possible by incorporating the proposed solution, whereas the variations of displacement are underestimated by assuming plastic behavior model used by Brown and Bray (1982).
- For the hydraulic analysis, the accurate non-radial Ming's model (Ming *et al*. 2010) was developed to model distribution of pore water pressure around the tunnel. Considering the results derived from Ming's model, compared to those obtained by Kolymbas and Wagner (2007) method and FLAC program, it was observed that Ming's model involves appropriate accuracy for analysis of seepage in shallow to deep underwater tunnels.
- It was shown that the flow of groundwater into tunnels results in significant effect on ground response curve. In comparison with dry condition, seepage flow into a tunnel induces seepage forces, and consequently increases the tunnel convergence.
- By increasing dilatancy angle, plastic strain rises in each loop which in turns leads to an increase in the displacements. Moreover, taking into account the effects of effective stress and seepage body forces, convergence of the tunnel enhances in comparison to the total stress method.
- In fact, gravitational loading differs for various directions around the tunnel. Taking into account the effect of gravitational loads on ground response curve, a greater deformation is obtained for tunnel crown as compared to its wall and floor.
- For determination of ground response curve at tunnel crown and floor, the effects of seepage and gravitational loads are needed to be considered simultaneously. Seepage acts upon increasing the deformation at all directions in tunnel periphery. Nevertheless, gravitational loads lead to an increase in displacement of tunnel crown and a decrease in displacement of floor; while they do not affect the ground response curve at tunnel wall. As the effects of

gravitational loads and the seepage forces in the analyses can be noticeable, ignoring each of them can lead to significant errors in the corresponding calculations.

References

Alonso, E., Alejano, L.R., Varas, F., Fdez-Manin, G. and Carranza-Torres, C. (2003), "Ground response curves for rock masses exhibiting strain-softening behavior", *Int. J. Numer. Anal. Method. Geomech.*, **27**(13), 1153-1185.

Brown, E.T. and Bray, J.W. (1982), "Rock-lining interaction calculations for pressure shafts and tunnels", *ISRM Symposium*, Aachen, Germany, pp. 26-28.

Brown, E.T., Bray, J.W., Ladanyi, B and Hoek, E. (1983), "Ground response curves for rock tunnels", *J. Geotech. Eng.*, **109**(1), 15-39.

Carranza-Torres, C. (2004), "Elasto-plastic solution of tunnel problems using the generalized form of the Hoek–Brown failure criterion", *Int. J. Rock. Mech. Min. Sci.*, **41**, 480-481.

Carranza-Torres, C. and Fairhurst, C. (1999), "On the stability of tunnels under gravity loading, with post-peak softening of the ground", *Int. J. Rock. Mech. Min. Sci.*, **34**(3-4), 75.e1–75.e18.

Detournay, E. and Fairhurst, C. (1987), "Two dimensional elastoplastic analysis of along, cylindrical cavity under non-hydrostatic loading", *Int. J. Rock. Mech. Min. Sci. Geomech. Abs.*, **24**(4), 197-211.

Fahimifar, A. and Zareifard, M.R. (2009), "A theoretical solution for analysis of tunnels below groundwater considering the hydraulic-mechanical coupling", *Tunn. Undergr. Sp. Tech.*, **24**(6), 634-646.

Fahimifar, A., Ghadami, H. and Ahmadvand, M. (2014), "The influence of seepage and gravitational loads on elastoplastic solution of circular tunnels", *Sci Iran.*, **21**(6), 1821-1832.

Fahimifar, A., Ghadami, H. and Ahmadvand, M. (2015), "An elasto-plastic model for underwater tunnels considering seepage body forces and strain-softening behaviour", *Eur. J. Environ. Civ. Eng.*, **19**(2), 129-151.

Fernandez, G. (1994), "Behavior of pressure tunnels and guidelines for liner design", *J. Geotech. Eng.*, **120**(10), 1768-1791.

Hoek, E. and Brown, E. (1980), "Empirical strength criterion for rock masses", *J. Geotech. Eng.*, **106**(GT9), 1013-1035.

Kolymbas, D. and Wagner, P. (2007), "Groundwater ingress to tunnels – the exact analytical solution", *Tunn. Undergr. Sp. Tech.*, **22**(1), 23-27.

Lee, Y-K. and Pietruszczak, S. (2008), "A new numerical procedure for elasto-plastic analysis of a circular opening excavated in a strain-softening rock mass", *Tunn. Undergr. Sp. Tech.*, **23**(5), 588-599.

Lee, S.W., Jung, J.W., Nam, S.W. and Lee, I.M. (2006), "The influence of seepage forces on ground reaction curve of circular opening", *Tunn. Undergr. Sp. Tech.*, **22**(1), 28-38.

Ming, H., Meng-Shu, W., Tan, Z-S. and Xiu-Ying, W. (2010), "Analytical solution for steady seepage into an underwater circular tunnel", *Tunn. Undergr. Sp. Tech.*, **25**(4), 391-396.

Park, K-H. and Kim, Y-J. (2006), "Analytical solution for a circular opening in, an elasto-brittle-plastic rock", *Int. J. Rock. Mech. Min. Sci.*, **43**(4), 616-622.

Park, K-H., Tontavanich, B. and Lee, J.-G. (2008), "A simple procedure for ground response Curve of circular tunnel in elastic-strain softening rock masses", *Tunn. Undergr. Sp. Tech.*, **23**(2), 151-159.

Sharan, S.K. (2003), "Elastic-brittle-plastic analysis of circular openings in Hoek-Brown media", *Int. J. Rock. Mech. Min. Sci.*, **40**(6), 817-824.

Sharan, S.K. (2005), "Exact and approximate solutions for displacements around circular openings in elastic-brittle-plastic Hoek-Brown rock", *Int. J. Rock. Mech. Min. Sci.*, **42**(4), 542-549.

Shin, J.H., Shin, Y.S., Kim, S.H. and Shin, H.S. (2007), "Evaluation of residual pore water pressures on linings for undersea tunnels", *Chin. J. Rock. Mech. Eng.*, **26**(2), 3682-3688.

Shin, Y.J., Kim, B.M., Shin, J.H. and Lee, I.M. (2010), "The ground reaction curve of underwater tunnels considering seepage forces", *Tunn. Undergr. Sp. Tech.*, **25**(4), 315-324.

Shin, J.H., Lee, I.M. and Shin, Y.J. (2011), "Elasto-plastic seepage-induced stresses due to tunneling", *Int. J.*

Numer. *Anal*. *Method*. *Geomech*., **35**(13), 1432-1450.
Skempton, A.W. (1961), "Effective stress in soils, concrete and rock", In: *Pore Pressure and Suction in Soils*, Butterworth, London, UK, pp. 4-16.
Terzaghi, K. (1923), "Die berechnung der durchlassigkeitsziffer des tones aus dem verlauf der hydrodynamischen spannungerscheinungen", Sitz. Akad. Wissen. Wien, Math. Naturwiss. Kl., Abt. IIa, **132**, 125-138.
Timoshenko, S.P. and Goodier, J.N. (1982), *Theory of Elasticity*, McGraw-Hill, New York, NY, USA.
Wang, Y. (1996), "Ground response of circular tunnel in poorly consolidated rock", *J*. *Geotech*. *Eng*., **122**(9), 703-708.
Zareifard, M.R. and Fahimifar, A. (2012), "A new solution for shallow and deep tunnels by considering the gravitational Loads", *Acta*. *Geotech*. *Slov*., **2012**(2).

CC

Nomenclature

r	radial distance from the center of the tunnel	r	depth of the tunnel from ground surface
θ	angle measured clockwise from horizontal direction	i_r	hydraulic gradient
σ_r	Radial stress	H_w	hydraulic head
σ_θ	circumferential stress	P_w	pore water pressure
σ_1	major principal stress	σ_o	initial stress
σ_3	minor principal stress	P_i	tunnel internal pressure
ε_r	radial strain	γ_w	specific weight of water
ε_θ	circumferential strain	R_w	external radius of the rock zone affected by the seepage
ε_1	major principal strain	η^*	parameter indicating the length of strain-softening zone in Alonso's method
ε_3	minor principal strain	η	strain-softening function
w	expresses parameters m, s, σ_c, ψ	α	parameter indicating the length of strain-softening zone in Brown's method
w_p	parameters m, s, σ_c, ψ for intact rock mass	F_r	body forces in radial direction
w_r	Parameters m, s, σ_c, ψ for broken rock mass	F_θ	body forces in circumferential direction
$\overline{w}$	Parameters m, s, σ_c, ψ for different elements	γ	specific weight of rock mass
m, s	Material constants of Hoek-Brown failure criterion	P_{wo}	Hydrostatic water pressure
ψ	dilatancy angle	**Superscripts**	
σ_c	uniaxial compressive strength of intact rock	p	refers to quantities corresponding to plastic zone
E	deformability modulus of rock mass	E	refers to quantities corresponding to elastic zone
υ	poisson's ratio of rock mass	Prime	Denotes effective stress
ϕ_p	friction angle	**Subscripts**	
a	exponential coefficient of Hoek-Brown criterion	e	refers to quantities corresponding to excavation
r_o	radius of tunnel	s	refers to quantities corresponding to seepage body forces
r_e	elastoplastic radius	in	refers to quantities corresponding to initial state

Appendix A: Stress-strain analysis in plastic zone

Using Eq. (21), the equilibrium equation in plastic zone is obtained as Eq. (A1)

$$\frac{d\sigma'_r}{dr}+\gamma_w\frac{dH_w}{dr}-\gamma\sin\theta=\frac{\{m\sigma'_r\sigma_c+s{\sigma_c}^2\}^{\frac{1}{2}}}{r} \tag{A1}$$

Since introducing a closed-form solution is impossible for solving the above differential equation, the equations are solved using the numerical solution of finite difference method (FDM). Using the numerical FDM solution of Eq. (A1), radial stress in each ring can be solved as Eq. (A2)

$$\sigma'_r(i)=\sigma'_r(i-1)-C+bt^2+t[b^2t^2+4b(i-1)-2b+C+4d]^{\frac{1}{2}} \tag{A2}$$

Where

$$\begin{aligned}
&t=\frac{r(i)-r(i-1)}{r(i)+r(i-1)}\\
&d=\bar{s}(i).{\bar{\sigma}_c}^2(i)\\
&b=\bar{m}(i).{\bar{\sigma}_c}^2(i)\\
&C=\gamma_w(H_w(i)-H_w(i-1))-\gamma\sin\theta(r(i)-r(i-1))\\
&\bar{m}(i)=\frac{1}{2}(m(i-1)+m(i))\\
&\bar{s}(i)=\frac{1}{2}(s(i-1)+s(i))\\
&\bar{\sigma}_c(i)=\frac{1}{2}(\bar{\sigma}_c(i-1)+\bar{\sigma}_c(i))
\end{aligned} \tag{A3}$$

To calculate radial and circumferential strains, deformation-strain relationships of the axisymmetric condition are used. Unlike the model proposed by Brown *et al*. (1983), which assumes a constant elastic strain throughout the plastic zone, the proposed model is able to calculate increments of the elastic strain separately. Accordingly, the total strain is divided into two components; elastic and plastic strains

$$\begin{Bmatrix}\varepsilon_r\\ \varepsilon_\theta\end{Bmatrix}=\begin{Bmatrix}\varepsilon_r^e\\ \varepsilon_\theta^e\end{Bmatrix}+\begin{Bmatrix}\varepsilon_r^p\\ \varepsilon_\theta^p\end{Bmatrix} \tag{A4}$$

By substituting Eq. (A4) into Eq. (11) and using numerical FDM solution, $\Delta\varepsilon_\theta^p(i)$ (increment of circumferential plastic strain) is obtained as Eq. (A5) (Fahimifar *et al*. 2014):

$$\Delta\varepsilon_\theta^p(i)=\frac{P_1}{P_2}$$

$$P_1=-\Delta\varepsilon_\theta^e(i)+t\left[\frac{1+\upsilon}{E}\left(\Delta\sigma_r'(i)-\Delta\sigma_\theta'(i)\right)+2\left(\varepsilon_r(i-1)-\varepsilon_\theta(i-1)\right)\right] \tag{A5}$$

$$P_2=1+t(K(i)+1)$$

Where

$$t=\frac{r(i)-r(i-1)}{r(i)+r(i-1)} \tag{A6}$$

$$K=\frac{1+\sin\psi}{1-\sin\psi} \tag{A7}$$

Where, ψ denotes dilatancy angle.

In Eq. (A5), $\varepsilon_\theta\,(i-1)$ and $\varepsilon_r\,(i-1)$ are circumferential and radial strains calculated in the previous loop $(i-1)$, respectively. Here, $\Delta\varepsilon_\theta^p(i)$ and $\Delta\varepsilon_r^p(i)$ (circumferential and radial elastic strain increments) also are obtained from Eq. (A8)

$$\begin{Bmatrix}\Delta\varepsilon_r^e(i)\\ \Delta\varepsilon_\theta^e(i)\end{Bmatrix}=\frac{1}{2G}\begin{bmatrix}1-\nu & -\nu\\ -\nu & 1-\nu\end{bmatrix}\begin{Bmatrix}\Delta\sigma_r'(i)\\ \Delta\sigma_\theta'(i)\end{Bmatrix}$$

$$\begin{Bmatrix}\Delta\sigma_r'(i)\\ \Delta\sigma_\theta'(i)\end{Bmatrix}=\begin{Bmatrix}\sigma_r'(i)-\sigma_r'(i-1)\\ \sigma_\theta'(i)-\sigma_\theta'(i-1)\end{Bmatrix} \tag{A8}$$

After calculating $\Delta\varepsilon_\theta^p(i)$ from Eq. (A5), $\Delta\varepsilon_r^p(i)$ can be derived from Eq. (A9)

$$\Delta\varepsilon_r^p(i)=-K(i)\Delta\varepsilon_\theta^p(i) \tag{A9}$$

Also, the strain-softening parameter (η) for each loop is estimated as Eq. (A10)

$$\eta(i)=\eta(i-1)+(\Delta\varepsilon_\theta^p(i)-\Delta\varepsilon_r^p(i)) \tag{A10}$$

In this step, the plastic strain can also be calculated using the parameters obtained from previous steps

$$\begin{cases}\varepsilon_r^p(i)=\varepsilon_r^p(i-1)+\Delta\varepsilon_r^p(i)\\ \varepsilon_\theta^p(i)=\varepsilon_\theta^p(i-1)+\Delta\varepsilon_\theta^p(i)\end{cases} \tag{A11}$$

And the total circumferential and radial strains are expressed as the sum of elastic and plastic strains using Eq. (A12)

$$\begin{Bmatrix} \varepsilon_r(i) \\ \varepsilon_\theta(i) \end{Bmatrix} = \begin{Bmatrix} \varepsilon_r(i-1) \\ \varepsilon_\theta(i-1) \end{Bmatrix} + \begin{Bmatrix} \Delta\varepsilon_r^e(i) \\ \Delta\varepsilon_\theta^e(i) \end{Bmatrix} + \begin{Bmatrix} \Delta\varepsilon_r^p(i) \\ \Delta\varepsilon_\theta^p(i) \end{Bmatrix} \tag{A12}$$

Finally, through calculating the total circumferential strain, deformation also can be obtained using Eq. (A13)

$$u(i) = -\varepsilon_\theta(i) r(i) \tag{A13}$$

To perform the analysis, by assuming an elasto-plastic radius (r_e), calculations are performed at the elasto-plastic boundary. Then, by taking the initial values for stress, stain and deformation obtained at the elasto-plastic boundary as initial values, equations of plastic zone are numerically solved until the value of the radial stress for a specific $r(n)$ (i.e., $\sigma_r'(n)$) reaches P_i. The calculations are continued until the analysis converges.

Appendix B: Stress-strain analysis in elastic zone

Based on Eq. (33), Eq. (B1) is obtained for deformation induced by seepage in elastic zone

$$\frac{d^2u_{r(s)}}{dr^2}+\frac{1}{r}\frac{du_{r(s)}}{dr}-\frac{u_{r(s)}}{r^2}=B\gamma_w\frac{dH_w}{dr} \tag{B1}$$

Where

$$B=\frac{(1+\upsilon)(1-2\upsilon)}{E(1-\upsilon)} \tag{B2}$$

Considering different boundary conditions and hydraulic head distributions at different directions around tunnel periphery, stress, strain, and deformation induced by seepage forces are obtained for horizontal and vertical directions as follows:

B.1 Horizontal direction ($\theta = 0°$, *Along the tunnel walls*)

Considering Eq. (13), hydraulic head distribution through horizontal direction ($\theta = 0°$) is obtained using Eq. (B3)

$$H_w(r,\theta=0)=\frac{P_w(r_o)/\gamma_w-h}{2\ln\left(\frac{h}{r_o}-\sqrt{\left(\frac{h}{r_o}\right)^2-1}\right)}\left(\ln\frac{r^2+(-h+\sqrt{h^2-r_o^2})^2}{r^2+(-h-\sqrt{h^2-r_o^2})^2}\right) \tag{B3}$$

By differentiating Eq. (B3), Eq. (B4) is obtained

$$\frac{dH_w}{dr}=A\frac{2r(S_1-S_2)}{\gamma_w(S_1+r^2)(S_2+r^2)} \tag{B4}$$

Where

$$A=\frac{P_w(r_o)-\gamma_w h}{2\ln\left[\frac{h}{r_o}-\sqrt{\left(\frac{h}{r_o}\right)^2-1}\right]} \tag{B5}$$

$$S_1=(-\sqrt{h^2-r_o^2}-h)^2 \tag{B6}$$

$$S_2=(\sqrt{h^2-r_o^2}-h)^2 \tag{B7}$$

By replacing the above equation for differentiation of hydraulic head in deformation Eq. (B1), Eq. (B8) is derived

$$\frac{d^2u_{r(s)}}{dr^2}+\frac{1}{r}\frac{du_{r(s)}}{dr}-\frac{u_{r(s)}}{r^2}=AB\frac{2r(S_1-S_2)}{(S_1+r^2)(S_2+r^2)} \tag{B8}$$

By solving Eq. (B8), deformation, strain, and stress induced by seepage forces along the horizontal direction in the elastic zone, are obtained through Eqs. (B9)- (B13)

$$u_{r(s)}=C_1r+\frac{C_2}{r}+AB\ln\frac{(S_2+r^2)^{(S_2+r^2)}}{(S_1+r^2)^{(S_1+r^2)}} \tag{B9}$$

$$\varepsilon_{r(s)}=-\frac{du_{r(s)}}{dr}=-C_1+\frac{C_2}{r^2}+\frac{AB}{2r^2}\ln\frac{(S_2+r^2)^{(S_2+r^2)}}{(S_1+r^2)^{(S_1+r^2)}}-AB\ln\frac{S_2+r^2}{S_1+r^2} \tag{B10}$$

$$\varepsilon_{\theta(s)}=-\frac{u_{r(s)}}{dr}=-C_1-\frac{C_2}{r^2}-\frac{AB}{2r^2}\ln\frac{(S_2+r^2)^{(S_2+r^2)}}{(S_1+r^2)^{(S_1+r^2)}} \tag{B11}$$

$$\sigma'_{r(s)}=\frac{E}{(1+\upsilon)(1-2\upsilon)}\left[(1-\upsilon)\varepsilon_{r(s)}+\upsilon\varepsilon_{\theta(s)}\right] \tag{B12}$$

$$\sigma'_{\theta(s)}=\frac{E}{(1+\upsilon)(1-2\upsilon)}\left[(1-\upsilon)\varepsilon_{\theta(s)}+\upsilon\varepsilon_{r(s)}\right] \tag{B13}$$

In Eqs. (B9)-(B13), constants C_1 and C_2 are obtained by applying the boundary conditions.

In the case of considering the range of seepage radius as infinite through horizontal direction, the boundary conditions are considered as Eq. (B14)

$$\left\{\begin{matrix}\sigma'_{r(s)}\left|r\to\infty\right|=0\\ \sigma'_{r(s)}\left|r=r_o\right|=0\end{matrix}\right\} \tag{B14}$$

By considering the boundary conditions according to Eq. (B14), constants C_1 and C_2 are obtained as Eqs. (B15)-(B16)

$$C_1=0 \tag{B15}$$

$$C_2=-\frac{AB}{2}\ln\frac{(S_2+r_o{}^2)^{(S_2+r_o{}^2)}}{(S_1+r_o{}^2)^{(S_1+r_o{}^2)}}+\frac{AB(1-\upsilon)r_o^2}{1-2\upsilon}\ln\frac{S_2+r_o{}^2}{S_1+r_o{}^2} \tag{B16}$$

When the range of seepage radius through horizontal direction is considered as a finite value (R_w), the boundary conditions are considered using Eq. (B17)

$$\left.\begin{matrix}\sigma'_{r(s)}\left|r=R_w\right|=0\\ \sigma'_{r(s)}\left|r=r_o\right|=0\end{matrix}\right\} \tag{B17}$$

By considering the boundary conditions according to Eq. (B17), constants C_1 and C_2 are derived as Eqs. (B18)-(B21)

$$C_2 = \frac{C_3}{C_4} \tag{B18}$$

$$\begin{aligned} C_3 = {} & \frac{AB(1-2\upsilon)}{2r_o^2}\ln\frac{(S_2+{r_o}^2)^{(S_2+{r_o}^2)}}{(S_1+{r_o}^2)^{(S_1+{r_o}^2)}} - \frac{AB(1-2\upsilon)}{2R_w^2}\ln\frac{(S_2+R_w^2)^{(S_2+R_w^2)}}{(S_1+R_w^2)^{(S_1+R_w^2)}} \\ & - AB(\upsilon-1)\left(\ln\frac{S_2+R_w^2}{S_1+R_w^2} - \ln\frac{S_2+{r_o}^2}{S_1+{r_o}^2}\right) \end{aligned} \tag{B19}$$

$$C_4 = (1-2\upsilon)\left(\frac{1}{R_w^2}-\frac{1}{r_o^2}\right) \tag{B20}$$

$$C_1 = -\frac{C_2}{R_w^2} - \frac{AB}{2R_w^2}\ln\frac{(S_2+R_w^2)^{(S_2+R_w^2)}}{(S_1+R_w^2)^{(S_1+R_w^2)}} \tag{B21}$$

B.2 Vertical direction (θ = 0°, Along the tunnel crown)

Considering Eq. (13), hydraulic head distribution through the direction (θ = 90°) (along the tunnel crown) is obtained using Eq. (B22)

$$H_w(r,\theta=90) = \frac{P_w(r_o)/\gamma_w + r_o - h}{2\ln\left(\frac{h}{r_o}-\sqrt{\left(\frac{h}{r_o}\right)^2-1}\right)}\left(\ln\frac{(r-h+\sqrt{h^2-{r_o}^2})^2}{(r-h-\sqrt{h^2-{r_o}^2})^2}\right) \tag{B22}$$

By differentiating Eq. (B22), Eq. (B23) is obtained

$$\frac{dH_w}{dr} = A\frac{2(S_1-S_2)}{\gamma_w(S_1+r)(S_2+r)} \tag{B23}$$

Where

$$A=\frac{P_w(r_o)+r_o-\gamma_w h}{2\ln\left[\frac{h}{r_o}-\sqrt{\left(\frac{h}{r_o}\right)^2-1}\right]} \tag{B24}$$

$$S_1=(-\sqrt{h^2-r_o^2}-h)^2 \tag{B25}$$

$$S_1=(\sqrt{h^2-r_o^2}-h)^2 \tag{B26}$$

By replacing the above equation for differentiation of pore water pressure in deformation Eq. (B1), Eq. (B27) is derived

$$\frac{d^2u_{r(s)}}{dr^2}+\frac{1}{r}\frac{du_{r(s)}}{dr}-\frac{u_{r(s)}}{r^2}=AB\frac{2(S_1-S_2)}{(S_1+r)(S_2+r)} \tag{B27}$$

Solving Eq. (B27), deformation, strain, and stress induced by seepage forces in the direction θ = 90° in the elastic zone are obtained through Eqs. (B28)-(B32)

$$u_{r(s)}=C_1r+\frac{C_2}{r}+\frac{AB}{2}\left[\ln\frac{r+S_2}{r+S_1}+(S_2-S_1)r+\ln\frac{(S_2+r)^{S_2}}{(S_1+r)^{S_1}}\right] \tag{B28}$$

$$\varepsilon_{r(s)}=-\frac{du_{r(s)}}{dr}=-C_1+\frac{C_2}{r^2}+\frac{AB}{2}\left[\frac{S_1-S_2}{(r+S_1)(r+S_2)}+(S_1-S_2)+\frac{S_1}{S_1+r}-\frac{S_2}{S_2+r}\right] \tag{B29}$$

$$\varepsilon_{\theta(s)}=-\frac{u_{r(s)}}{r}=-C_1-\frac{C_2}{r^2}-\frac{AB}{2r}\left[\ln\frac{r+S_2}{r+S_1}+(S_2-S_1)r+\ln\frac{(S_2+r)^{S_2}}{(S_1+r)^{S_1}}\right] \tag{B30}$$

$$\sigma'_{r(s)}=\frac{E}{(1+\upsilon)(1-2\upsilon)}\left[(1-\upsilon)\varepsilon_{r(s)}+\upsilon\varepsilon_{\theta(s)}\right] \tag{B31}$$

$$\sigma'_{\theta(s)}=\frac{E}{(1+\upsilon)(1-2\upsilon)}\left[(1-\upsilon)\varepsilon_{\theta(s)}+\upsilon\varepsilon_{r(s)}\right] \tag{B32}$$

In Eqs. (B28)-(B32), constants C_1 and C_2 are obtained by applying the boundary conditions. When the range of seepage radius is considered as a finite value (R_w) in the direction θ = 90°, the boundary conditions are considered using Eq. (B17)

$$\left.\begin{matrix}\sigma'_{r(s)}|r=R_w|=0\\ \sigma'_{r(s)}|r=r_o|=0\end{matrix}\right\} \tag{B17}$$

By considering the boundary conditions according to Eq. (B17), constants C_1 and C_2 are derived as Eqs. (B33)-(B34)

$$C_1=-\frac{C_2}{{r_o}^2}(2\upsilon-1)+\frac{AB}{2}\left[\begin{matrix}\frac{(S_1-S_2)(1-\upsilon)}{(r_o+S_1)(r_o+S_2)}+(S_1-S_2)\\ +(1-\upsilon)\frac{S_2}{(S_2+r_o)(S_1+r_o)}-\frac{\upsilon}{r_o}\ln\frac{(r_o+S_2)^{(S_2+1)}}{(r_o+S_1)^{(S_1+1)}}\end{matrix}\right] \tag{B33}$$

$$C_2=\frac{ABr_o^2h^2}{2(2\upsilon-1)(r_o^2-h^2)}\left[\begin{matrix}\frac{(S_1-S_2)(1-\upsilon)}{(h+S_1)(h+S_2)}-\frac{(S_1-S_2)(1-\upsilon)}{(r_o+S_2)(r_o+S_1)}\\ +(1-\upsilon)\left(\frac{S_1}{S_1+h}-\frac{S_2}{S_2+h}\right)-(1-\upsilon)\left(\frac{S_1}{S_1+r_o}-\frac{S_2}{S_2+r_o}\right)\\ -\frac{\upsilon}{h}\ln\frac{(h+S_2)^{(S_2+1)}}{(h+S_1)^{(S_1+1)}}+\frac{\upsilon}{r_o}\ln\frac{(r_o+S_2)^{(S_2+1)}}{(r_o+S_1)^{(S_1+1)}}\end{matrix}\right] \tag{B34}$$

B.3 Vertical direction (θ = 270°, Along the tunnel floor)

Considering Eq. (13), hydraulic head distribution through the direction $\theta = 270°$ (along the tunnel floor) is obtained using Eq. (B35)

$$H_w(r,\theta=270)=\frac{P_w(r_o)/\gamma_w-r_o-h}{2\ln\left(\frac{h}{r_o}-\sqrt{\left(\frac{h}{r_o}\right)^2-1}\right)}\left(\ln\frac{(-r-h+\sqrt{h^2-{r_o}^2})^2}{(-r-h-\sqrt{h^2-{r_o}^2})^2}\right) \tag{B35}$$

By differentiating Eq. (B35), Eq. (B36) is obtained

$$\frac{dH_w}{dr}=A\frac{2(S_2-S_1)}{\gamma_w(r-S_1)(r-S_2)} \tag{B36}$$

Where

$$A=\frac{P_w(r_o)-r_o-\gamma_w h}{2\ln\left[\frac{h}{r_o}-\sqrt{\left(\frac{h}{r_o}\right)^2-1}\right]} \tag{B37}$$

$$S_1 = (-\sqrt{h^2 - r_o^2} - h)^2 \tag{B38}$$

$$S_1 = (\sqrt{h^2 - r_o^2} - h)^2 \tag{B39}$$

By replacing the above equation in deformation Eq. (B1), Eq. (B40) is derived

$$\frac{d^2 u_{r(s)}}{dr^2} + \frac{1}{r}\frac{du_{r(s)}}{dr} - \frac{u_{r(s)}}{r^2} = AB\frac{2(S_{21} - S_1)}{(r - S_1)(r - S_2)} \tag{B40}$$

Solving Eq. (B40), deformation, strain, and stress induced by seepage through the direction θ = 270° in the elastic zone are obtained through Eqs. (B41)-(B45)

$$u_{r(s)} = C_1 r + \frac{C_2}{r} + \frac{AB}{2}\left[\ln\frac{r - S_2}{r - S_1} + (S_1 - S_2)r + \ln\frac{(r - S_1)^{S_1}}{(r - S_2)^{S_2}}\right] \tag{B41}$$

$$\varepsilon_{r(s)} = -\frac{du_{r(s)}}{dr} = -C_1 + \frac{C_2}{r^2} + \frac{AB}{2}\left[\frac{S_1 - S_2}{(r - S_1)(r - S_2)} + (S_2 - S_1) + \frac{S_1}{r - S_1} - \frac{S_2}{r - S_2}\right] \tag{B42}$$

$$\varepsilon_{\theta(s)} = -\frac{u_{r(s)}}{r} = -C_1 - \frac{C_2}{r^2} - \frac{AB}{2r}\left[\ln\frac{r - S_2}{r - S_1} + (S_1 - S_2)r + \ln\frac{(r - S_1)^{S_1}}{(r - S_2)^{S_2}}\right] \tag{B43}$$

$$\sigma'_{r(s)} = \frac{E}{(1+\upsilon)(1-2\upsilon)}\left[(1-\upsilon)\varepsilon_{r(s)} + \upsilon\varepsilon_{\theta(s)}\right] \tag{B44}$$

$$\sigma'_{\theta(s)} = \frac{E}{(1+\upsilon)(1-2\upsilon)}\left[(1-\upsilon)\varepsilon_{\theta(s)} + \upsilon\varepsilon_{r(s)}\right] \tag{B45}$$

In Eqs. (B41)-(B45), constants C_1 and C_2 are obtained through applying the boundary conditions.
In the case of considering the range of seepage radius as infinite through the direction θ = 270°, the boundary conditions are considered as Eq. (B14)

$$\left\{\begin{matrix}\sigma'_{r(s)}\left|r \to \infty\right| = 0\\ \sigma'_{r(s)}\left|r = r_o\right| = 0\end{matrix}\right\} \tag{B14}$$

By considering the boundary conditions according to Eq. (B14), constants C_1 and C_2 are obtained as Eqs. (B46)-(B47)

$$C_1 = \frac{AB}{2}(S_2 - S_1) \tag{B46}$$

$$C_2 = \frac{ABr_o^2}{2(2\upsilon - 1)}\left[\frac{(S_1 - S_2)(1-\upsilon)}{(r_o - S_2)(r_o - S_1)} - (1-\upsilon)\left(\frac{S_1}{r_o - S_1} - \frac{S_2}{r_o - S_2}\right) + \frac{\upsilon}{r_o}\ln\frac{(r_o - S_2)^{(S_2 - 1)}}{(r_o - S_1)^{(S_1 - 1)}}\right] \tag{B47}$$

Appendix C: Stresses and strains induced by the tunnel excavation in elastic zone

Based on Eq. (38), Eq. (C1) is obtained for deformation induced by the tunnel excavation in elastic zone

$$\frac{d^2u_{r(e)}}{dr^2}+\frac{1}{r}\frac{du_{r(e)}}{dr}-\frac{u_{r(e)}}{r^2}=0 \tag{C1}$$

The differential Eq. (C1) can be solved using the boundary conditions in the interior and exterior boundaries of the elastic zone. Considering the boundary conditions as $\sigma'_{r(e)}=\sigma'_{r(e)}(r_e)$ in $r = r_e$ and $\sigma'_{r(e)}=0$ in $r\to\infty$ stresses, strains and deformation induced by excavation can be calculated using Eqs. (C2)-(C4) (Zareifard and Fahimifar 2012)

$$\varepsilon_{r(e)}(r)=-\varepsilon_{\theta(e)}(r)=\frac{1+\upsilon}{E}\left[\sigma'_{r(e)}(r_e)\right]\left(\frac{r_e}{r}\right)^2 \tag{C2}$$

$$\sigma'_{r(e)}(r)=-\sigma'_{\theta(e)}(r)=\left[\sigma'_{r(e)}(r_e)\right]\left(\frac{r_e}{r}\right)^2 \tag{C3}$$

$$u_{r(e)}(r)=\frac{1+\upsilon}{E}\left[\sigma'_{r(e)}(r_e)\right]\frac{r_e^2}{r} \tag{C4}$$

Where $\sigma'_{r(e)}(r_e)$ is the radial stress induced by the tunnel excavation at the elasto-plastic boundary and is obtained using Eq. (C5)

$$\sigma'_{r(e)}(r_e)=\sigma'_r(r_e)-\sigma'_{r(s)}(r_e)-\sigma'_o \tag{C5}$$

The total stresses at the elasto-plastic boundary $\sigma'_{\theta(e)}(r_e)$ and $\sigma'_r(r_e)$ must satisfy the failure criterion. Thus, by substituting in the Hoek-Brown failure criterion and solving the derived equation, total radial stress at the elasto-plastic boundary is obtained as Eq. (C6)

$$\sigma'_{r(e)}(r_e)=\frac{1}{2}\left[A_1+A_2-\sqrt{(A_1)^2+2A_1A_2+A_3}\right] \tag{C6}$$

Where

$$A_2=\frac{m\sigma_c}{4} \tag{C8}$$

$$A_3=s\sigma_c^2 \tag{C9}$$

$$A_1=\sigma'_{r(s)}(r_e)+\sigma'_{\theta(s)}(r_e)+2\sigma'_o \tag{C7}$$